August 19, 1975

To the Graduate Council:

I am submitting herewith a thesis written by Carol Lynn Mason entitled "Vaporization of Water Droplets in High Temperature Air Streams." I recommend that it be accepted in partial fulfillment of the requirements for the degree of Master of Science, with a major in Chemical Engineering.

George C. Frazier

George C. Frazier, Major Professor

We have read this thesis and recommend its acceptance:

Oran L. Culberson

J. A. Watson

Accepted for the Council:

Hilton A. Smith

Vice Chancellor
Graduate Studies and Research

A

VAPORIZATION OF WATER DROPLETS IN HIGH TEMPERATURE AIR STREAMS

A Thesis

Presented for the

Master of Science

Degree

The University of Tennessee

Carol Lynn Mason

December 1975

1266313

ABSTRACT

An experiment was conducted to measure the vaporization rates of small, uniform water droplets moving under forced convection through a hot air stream. The experimental data were to provide sufficient information to establish a correlation between vaporization rate and droplet Reynolds number over a range of air stream temperatures.

The experimental method was based on the photographic observation of a well-defined stream of small water droplets directed through the center of an elevated temperature air stream. Droplet diameters ranged from 266-296 microns and droplet Reynolds numbers ranged from 7.56 to 14.60. The temperatures of the air stream ranged from 684 to 868°C. Vaporization rates obtained ranged from 55.0×10^{-6} to 173.8×10^{-6} gm/sec.

Although the data obtained exhibited a significant degree of scatter, it was found that the vaporization rates were markedly higher than those reported by previous workers for stationary suspended droplets at lower temperature ranges. The vaporization rate-Reynolds number correlation, although not statistically significant, showed a greater dependence on Reynolds number than had been determined for the case of suspended droplets. Several factors in addition to forced convection which could have influenced the vaporization rates were considered and it was concluded that they were either too small to have affected the results or that there was insufficient data to establish their significance.

Finally, it was concluded that the experimental method was valid

for studying the effects of forced convection on small droplets in high temperature air streams. Several recommendations for refinements in experimental design which might increase the range of useful data and decrease the experimental error were also provided.

TABLE OF CONTENTS

CHAPTER	PAGE
I. INTRODUCTION	1
II. THEORY	4
III. LITERATURE SURVEY	7
IV. EXPERIMENTAL APPARATUS AND PROCEDURE	21
V. RESULTS AND INTERPRETATION	29
VI. CONCLUSIONS AND RECOMMENDATIONS	50
LIST OF REFERENCES	54
APPENDICES	57
Appendix A	58
Appendix B	62
Appendix C	64
Appendix D	67
Appendix E	69
VITA	71

LIST OF FIGURES

FIGURE		PAGE
1.	Experimental Setup	22
2.	Droplet Generating Assembly	23
3.	Photograph of a Typical Plate	32
4.	Microdensitometer Trace of a Single Droplet	33
5.	Droplet Spacing for a Typical Run	36
6.	Typical Temperature Profile	38
7.	Variation of d^2 with Time	40
8.	Droplet Reynolds Number Dependence of Vaporization Rate	44
9.	Photograph of a Plate Showing Slightly Elongated Droplets	48
10.	Microdensitometer Trace of the Wire Image	63
11.	Droplet Spacing Correlations	65
12.	Temperature Profiles	70

CHAPTER I

INTRODUCTION

Vaporization of liquid droplets in gaseous media is a process encountered in many engineering problems and physical situations including spray towers, fogs, combustors, and engines using liquid fuels. In particular, the vaporization rate of small fuel droplets may be the rate limiting step in the total combustion process in some applications. As a result, attencion has been focused on various aspects of the vaporization process. In spite of the interest in this problem, however, there has yet to be developed a reasonably general design correlation for the vaporization process which is applicable to a wide variety of situations and which can be supported experimentally.

Some empirical correlations have been developed for specific physical situations and limited ranges of data. However, the difficulty of the general problem becomes apparent when one considers the dynamics of simultaneous heat and mass transfer which are involved. The problem is especially difficult for rapid vaporization in high temperature air streams because of the dependence of heat and mass transfer coefficients on high mass transfer rates occurring at high temperatures. The problem is further complicated by the determination of the range in vaporization rates and droplet sizes over which quasi-steady state may be considered a good approximation. In light of the difficulties associated with the analytical and

theoretical solution to this problem, quantitative data are desirable over a wide range of experimental conditions.

At least two experimental difficulties must be overcome in the quantitative study of vaporization of small droplets (less than several hundred microns). First, droplets in sprays are not of uniform size. Thus there is the problem of determining the size distribution function. Secondly, the droplets must either be fixed in space or their motion stopped photographically. Experiments in which the droplets are fixed have been carried out, but this tends to produce a lower limit on the size range that can be studied. Also, the extent to which the droplet holder affects the results is not readily known.

The experimental approach described here is an attempt to provide vaporization data on uniform droplets moving under forced convection through a hot air stream. This case corresponds most closely to actual operating situations but has been studied the least experimentally. By using this approach, the difficulties associated with stationary droplets and non-uniform droplets in sprays can be minimized. The experiment is based on the photographic observation of a well-defined stream of small droplets generated by induced breakup of a liquid jet coming from a fine capillary tube. Vaporization studies are made by directing the droplet stream in a horizontal direction through the center of an elevated, known temperature air stream near the exit of a tubular furnace. Data obtained consisted of the change in droplet diameter with time and vaporization rates

for moving droplets over a range of temperatures. This technique is particularly useful because it can provide data on droplets of varying sizes and velocities and over a wide range of air temperatures and flow rates.

CHAPTER II

THEORY

A reasonably general correlation for the vaporization rate of a single droplet in a moving medium might take the form (8):

$$\dot{m} = \dot{m}_o \, [1 + f(Re, Sc)] \qquad (1)$$

where $\dot{m}$ is the droplet vaporization rate and $\dot{m}_o$ is the vaporization rate of the same droplet that would occur in an identical medium but under conditions of no motion relative to the droplet. The function f(Re, Sc) is a correction factor for the forced convection of the medium relative to the droplet. The form of Equation (1) is useful because it is possible to calculate $\dot{m}_o$ directly from first principles and a suitable model for a given situation. At the present time, however, the form of f(Re, Sc) must be deduced from experimental data because of the complex nature of the hydrodynamic processes which occur during vaporization. This is the approach followed in this work. Values of $\dot{m}_o$ calculated from theory are combined with experimentally determined values of $\dot{m}$ to establish experimentally the form of f(Re, Sc).

A suitable model for determining $\dot{m}_o$ consists of a spherical liquid droplet of radius, r, having a uniform temperature, T_s. The droplet is suspended in a gaseous medium of temperature T_∞ which is stagnant relative to the droplet. For the case of quasi-steady vaporization and binary diffusion of the vapor through the stagnant film

of the surrounding gaseous medium, the governing differential energy and mass conservation equations can be solved to obtain

$$\exp\left(-\frac{\dot{m}_o \bar{c}_{pA}}{4\pi r \bar{k}_m}\right) = \frac{1 - \dfrac{4\pi r^2 q_s^r}{\dot{m}_o \lambda_A}}{1 - \dfrac{4\pi r^2 q_s^r}{\dot{m}_o \lambda_A} + \alpha(\theta_\infty - \theta_s)} \tag{2}$$

and

$$\frac{1 - x_{As}}{1 - x_{A\infty}} = \left[\frac{1 - \dfrac{4\pi r^2 q_s^r}{\dot{m}_o \lambda_A}}{1 - \dfrac{4\pi r^2 q_s^r}{\dot{m}_o \lambda_A} + \alpha(\theta_\infty - \theta_s)}\right]^{Le'} \tag{3}$$

Equations (2) and (3) were developed by Frazier and Chang (6) by approximating the physical properties in terms of their mean values in the temperature and composition ranges of interest. By assuming that the vaporization is a quasi-equilibrium process, that the vapor and the gaseous medium both behave as ideal gases, and that the specific volume of the liquid is small relative to that of the vapor, the integrated form of the Clausius-Clapeyron equation can be used to relate x_{As}, the vapor mole fraction at the droplet surface, and θ_s, the normalized droplet surface temperature:

$$\frac{p_A}{p_t} \equiv x_{As} \simeq \frac{p_a}{p_t} \left[-\beta\left(\frac{1}{\theta_s} - 1\right)\right] \tag{4}$$

Equations (2) through (4) can be solved numerically for $\dot{m}_o$ for a droplet of radius r and a given normalized temperature θ_∞ far from the droplet, once the physical properties of the system are specified.

The droplet vaporization rate in the moving medium is related to the rate of decrease of droplet size by

$$\dot{m} = -\frac{d}{dt}\left(\frac{4}{3}\pi r^3 \rho_\ell\right) \tag{5}$$

Equation (5) can be rewritten in the form

$$\frac{d(d^2)}{dt} = -\frac{2\dot{m}}{\pi r_o \rho_\ell} \tag{6}$$

Thus the only data required to determine $\dot{m}$ experimentally consists of the change in droplet diameter with time plus appropriate property values. Previous experiments (22) have shown that d^2 is related linearly to the time required for the droplet to vaporize from an initial diameter d_o to a diameter d by the mass rate of vaporization $\dot{m}$. In the experimental work discussed here, values of $\dot{m}$ are determined from the change in droplet diameter with time and used with calculated values of $\dot{m}_o$ to determine the functional form of f(Re, Sc).

CHAPTER III

LITERATURE SURVEY

Three different experimental techniques have been devised for studying the vaporization and/or burning of a fuel droplet in an oxidizing (usually air) atmosphere (23). In the first technique (Class I), fuel is supplied internally to a stationary porous sphere at a steady rate which is just sufficient to maintain a liquid film on the surface of the sphere during vaporization. In the second technique (Class II), fuel droplets are suspended on stationary quartz fibers and the rate of decrease of the diameter of the droplet is measured both during vaporization and after ignition. In the third technique (Class III), small freely falling fuel droplets are ignited and observed during burning. Each of the techniques possesses certain intrinsic advantages over the others; for example, the first is steady state, the second yields accurate results for the diameter as a function of time, and the third is applicable to very small droplets. A summary of several experiments in this field and the class of experiment to which they belong is shown in Table I.

All of these experiments were attempts to study the phenomena which are excluded by the assumptions given in the last chapter in deriving the expression for $\dot{m}_o$. These phenomena are generally too complex to be included in accurate theoretical vaporization rate analyses. They require semi-empirical or experimental methods in deriving vaporization rate formulae.

TABLE I

EXPERIMENTS FOR STUDYING THE VAPORIZATION OF FUEL DROPLETS

Investigator	Class of Experiment
Frossling	II
Ranz and Marshall	II
Godsave	II
Hall and Diederichsen	II
Spalding	I
Hottel, Williams, and Simpson	III
Wise, Lorrell, and Wood	I
Kobayasi	II
Nishiwaki	II
Ingebo	III
Agoston, Wise, and Rosser	I
Bolt and Saad	III
Kumagai and Isoda	III
Hoffman and Gauvin	II

The most important phenomenon of this kind is forced convective motion of the gas relative to the droplet. This effect was first analyzed by Frossling for a vaporizing droplet (8). He did both theoretical and experimental work on the vaporization of aniline and water droplets in moving and in still air. He found that the ratio of the vaporization rate $\dot{m}$ to the vaporization rate without convection $\dot{m}_o$ is

$$\dot{m}/\dot{m}_o = 1 + 0.276\ Re^{1/2}Sc^{1/3} \qquad (7)$$

where Sc is the Schmidt number of the gas and Re is the Reynolds number of the droplet relative to the gas far upstream of the droplet.

Ranz and Marshall (17) reported a fundamental study of the factors influencing the rate of vaporization of water drops containing dissolved and suspended solids. The study was restricted to a droplet Reynolds number range of 0 to 200. Independent correlations of heat and mass transfer rates were obtained from drop temperatures measured with 1/2 mil thermocouples. Drop diameters ranged from 0.06 to 0.11 centimeters, and the air temperature, up to 220°C.

Rates of vaporization and heat transfer were obtained by Ranz and Marshall using a microtechnique in which drops of about one millimeter in diameter were suspended from a microburette in a vertical, upward flowing stream of air. Vaporization rates were determined by measuring the rate of feed through a burette necessary to maintain a constant drop diameter. The temperature of the drop and the air stream were measured with small thermocouples. Vaporization rates in still air

were determined in a special dryer. Suspended drops with decreasing diameter were evaporated in hot air streams and in still air. The rate of vaporization was observed through a microscope and recorded on motion picture film.

Equations for the heat and mass transfer correlations for vaporizing water drops obtained by Ranz and Marshall were:

$$Nu = 2.0 + 0.60\ Re^{1/2}Pr^{1/3} \tag{8}$$

$$Nu' = 2.0 + 0.60\ Re^{1/2}Sc^{1/3}. \tag{9}$$

Values of Nu for drops vaporizing in hot air were calculated making four assumptions:

1. T_{av} was the average temperature in the transfer path at which the thermal conductivity was taken;

2. The drop was considered to be spherical with all of its surface available for transfer;

3. In estimating thermal conductivity, the transfer path was considered to contain only air;

4. The main air stream was considered to be of uniform temperature and velocity distribution.

The experimental correlation for heat transfer extrapolated close to the theoretical minimum value of Nu = 2.0 at Re = 0. Data for mass transfer showed a greater slope and a lower intercept, but the difference was always less than 10 percent and usually much less than 5 percent. Some factors which may have contributed to errors in the

data and anomalies in the heat and mass transfer analogy were:

1. Inaccurate values of diffusivity;

2. p_A may not have been the saturation vapor pressure;

3. The partial pressure of water vapor in the air may not have been constant at low air rates where the air stream velocity and the velocity of free convection were of the same order of magnitude and the water vapor from the room air diffused into the jet;

4. Free convection may have been significant at low values of the air velocity.

Godsave (9) reported an investigation into the factors governing the rates of decrease in size of the drops in a liquid fuel spray during vaporization and combustion. The experimental technique was to suspend a single drop of fuel on a fine silica filament and to measure photographically the rate of decrease in size during combustion in still air. Two distinct mechanisms were proposed as determining the rates of decrease in size. The first occurred when the temperature of the ambient atmosphere was essentially the same as that of the individual drops and was low in relation to the boiling point of the fuel. In this case, the vaporization rate was determined by diffusion processes with vapor pressure being the predominant fuel parameter. The second mechanism occurred when there was a considerable difference in temperature between the drop and the surrounding atmosphere such as during high temperature vaporization and combustion. Godsave's experiments were concerned with the second mechanism and his results showed that the rate of decrease in size was determined by the rate of heat transfer to

the drop. When a drop was evaporating at high temperatures, the heat transfer to the drop was occurring in the presence of simultaneous evaporative mass transfer of the vapor. Thus the process of heat transfer depended on the equations for mass transfer in a moving medium.

Hall and Diederichsen (10) determined the rate of vaporization of water drops in a flame at pressures up to 20 atmospheres. For a drop diameter of 1000 μ, they found that the mass rate of vaporization was still proportional to the first power of the drop diameter which can be shown from Equation (2) for the case of negligible radiation.

The mass transfer equation was solved by Spalding (20) for the case of a sphere evaporating into a laminar gas stream. Mass transfer occurred at a rate determined by

$$\frac{\dot{m} d c_p}{k_g B} = f(B, Pr)\ Re^{1/2} \qquad (10)$$

where B is the transfer number determined from the fundamental balance equations. For the case of vaporization without combustion, the heat conservation and mass conservation equations apply independently and lead to two transfer numbers which must be numerically equal in any given case. A value of B = 0.77 was determined for water vaporizing into a gas stream at 2000°C. The relation between the transfer rate and the transfer number was represented by a plot of Nu/Nu' as a function of B where Nu is the value for simple heat transfer in the same circumstances and Nu' is the value for mass transfer.

Spalding's experimental method was to cause liquid fuel to flow continuously over the surface of a solid body of suitable form with any excess of fuel supplied over fuel burned being withdrawn continuously from the lowest point of the body. The burning rate was determined by measuring the amount of excess fuel. The measured combustion rate was plotted in dimensionless form $(\dot{m}/d\mu)/Re^{1/2}$ against B. Two conclusions were drawn on the basis of the experiments:

1. The relation between combustion rate and transfer number derived for the flat plate in longitudinal laminar flow was in good agreement with experiments performed on spheres in forced convection over a range of B from 0.6 to 5.0 and of droplet Reynolds number from 800 to 4000.

2. Over the same range, the experimental data may also be adequately correlated by the empirical relation

$$\dot{m}/d\mu = 0.53\ B^{3/5}\ Re^{1/2}. \qquad (11)$$

Hottel, Williams, and Simpson (12) studied droplet burning by projecting a stream of uniform droplets up into an electric furnace and allowing these droplets to follow their trajectories inside the furnace and out through the bottom. Residence time of the droplets in the furnace was measured photoelectrically. The degree of combustion of the droplets was found directly from the mass of the residual droplets. Combustion curves of six hydrocarbons all took the same form. First there was preheating to such a temperature that significant vaporization occurred followed by rapid vaporization in which the droplet was surrounded by a flame envelope formed by the burning hydrocarbons. The rate of consumption of the droplets was probably controlled by the

heat transfer rate to the droplet. Estimates of preheat time (time required for the surface of the droplet to reach boiling temperature) were compared with the experimental combustion curves. The experimental curves were not in disagreement with the calculated preheat times, although the data are not precise enough to validate the assumed heat transfer model. The slope of the curves $m^{2/3}$ versus time, t, was proportional to the group $(\dot{m}/4\pi r)$. All the experimental points could, within experimental error, be represented by straight lines, the slopes of which were independent of initial droplet diameter. A semi-empirical correlation for predicting vaporization rates which included the effect of the motion of the droplet was proposed:

$$\frac{\dot{m}}{4\pi r} = f(k_g/c_p) \ln (1 + B) \{1 + a(Re)^p (Sc)^q\}. \qquad (12)$$

Conditions of steady state combustion of a stationary droplet were obtained experimentally by Wise, Lorrell, and Wood (24) by feeding liquid reactant into a porous sphere at a rate determined by the physical and chemical parameters of the system under study. A measured gas stream flowed past the liquid body, thereby replenishing gaseous reactant and removing combustion products from the homogeneous vapor phase burning zone. The linear variation of mass burning rate, $\dot{m}$, with droplet radius was found to apply to droplets as large as 600 microns in radius. For the system ethyl alcohol-air, the slope of the curve yielded an evaporation constant about 15 percent higher than that reported by Godsave for measurements carried out under non-steady

state conditions. This might have been partially due to the imposed gas velocity flowing past the sphere. Also, the higher absorptivity of the porous sphere relative to that of the liquid resulted in a larger contribution of radiative heat transfer.

Examination of the experimental results indicated that a sphericosymmetric model qualitatively predicted the variation of the burning rate as a function of the droplet radius and the chemical properties of the system. The inadequacy of the model was demonstrated by the change in burning rate with total pressure. The model suggested that $\dot{m}$ was independent of pressure whereas previous work (10) demonstrated a weak dependence on pressure. This discrepancy might in part be attributed to the contribution of axial convection to the transport properties of the system. This effect may be introduced into the theoretical analysis by replacing the parameters for diffusive transport of mass and energy with appropriate mass and heat transfer coefficients which include free convective flow in an axial direction. Earlier experimental work showed that the empirical pressure exponent for the mass burning rate suggested the contribution of free convection to the overall process of heat transfer.

Kobayasi (14) studied by means of motion picture recordings the combustion mechanism of a fuel droplet suspended from a quartz fiber. The relation between the droplet diameter and the time for combustion at constant air temperature was given by

$$\frac{d(d^2)}{dt} = \text{constant} = -C_b \qquad (13)$$

which was similar to the equation for evaporation but with a greater slope. The conclusion was that for a volatile fuel the law of evaporation holds at the surface of the burning droplet with diffusion of a suitable vapor-air mixture from the droplet to the outer flame.

A similar study on the evaporation and ignition lag of fuel droplets at various ambient air temperatures observed by photographic methods was reported by Nishiwaki (16). A fuel droplet suspended from a silica filament was quickly introduced into a combustion chamber which was heated rapidly. The rates of evaporation were obtained from shadow photographs taken with a motion picture camera. An equation for calculating dr/dt was derived:

$$-r\frac{dr}{dt} = \frac{2}{\rho_\ell \{2\lambda_A + c_p(T_\infty - T_s)\}} \cdot \{\frac{k_g(T_\infty - T_s)}{(1-r/r_o)} + r\sigma\varepsilon(T_w^4 - T_s^4)\}. \quad (14)$$

Observed values of $k_1 = -(d(2r_o)^2/dt) = -(d(d)^2/dt)$ were plotted against $(T_\infty - T_b)$ and compared with values calculated from Equation (14).

Evaporation rates of liquid droplets, including water, in hot air streams were also studied using a similar method. It was determined that $d^{1.5}$ varied linearly with time during steady evaporation. For this case it was assumed that $4\pi r^2\sigma\varepsilon(T_w^4 - T_s^4)\, dt = 0$ and $(dT_s/dt) \simeq 0$. Then

$$(1 - \frac{r}{r_o})\, r\frac{dr}{dt} = \frac{k_g}{\rho_\ell c_p} \ln\{1 + \frac{c_p}{\lambda_A}(T_\infty - T_s)\} \quad (15)$$

Observed values of $(d(d^{1.5})/dt)$ were compared with the values calculated from Equation (15). Accurate values of t were difficult to obtain because T_s was found to vary with Re. The rates of heat transfer were higher than the corresponding values for solid spheres.

Ingebo (13) studied droplet sizes and acceleration rates in high velocity streams with a high speed camera. The camera utilized a rotating mirror which tracked the droplets and stopped the motion of their images on the film. The droplets were produced by an atomizer. Vaporization rates were calculated from the experimentally determined droplet size distribution, drag coefficients, and heat transfer coefficients, and heat transfer coefficients determined with pure liquids evaporating from the surface of porous spheres. The expression used to calculate the vaporization rate was

$$\frac{dm}{dt} = \frac{\pi d\, k_g (T_\infty / T_s)}{\lambda_A} \left[2 + (2.58 \times 10^6)\, (ReSc)^{0.6} \left(\frac{k_g}{k_m}\right)^{0.5} \right] \qquad (16)$$

The effects of forced convection and turbulence on droplet combustion were investigated by Agoston, Wise, and Rosser (1). A porous sphere, wetted with fuel and surrounded by a flame envelope in a gas stream, was employed to simulate a burning droplet. Contributions to the vaporization rate from internal circulation and from droplet deformation from spherical shape which may occur under conditions of forced convection and turbulence were not taken into account in this experiment. The relationship tested was

$$\frac{\dot{m} - \dot{m}_o}{\dot{m}_o} = K\, Re^{1/2} \qquad (17)$$

where $\dot{m}_o$ was the theoretical mass burning rate without convection based on a sphericosymmetric model. The constant K was found to have the value 0.28 for ethyl alcohol and 0.20 for n-butyl alcohol. The difference in K may have been due partly to the values chosen for the fluid properties. Wide variations in turbulence intensity and scale had negligible effect on the mass burning rate.

Bolt and Saad (3) studied the combustion of individual fuel droplets falling freely in a hot atmosphere under controlled temperatures. Each drop was photographed at several positions as it fell through a heated furnace and a record of drop diameter and elapsed time was obtained. The coefficient of combustion, C_b, was taken from the equation

$$d^2 = d_o^2 - C_b t. \qquad (18)$$

It was a function of Nu, and in the case of small stationary drops or drops moving at a constant Reynolds number, Nu and C_b should be constant. In this case, however, the Reynolds number of the freely falling drop was continuously changing as both the velocity and the diameter changed. Thus Nu was not constant. This was believed to be the reason why the variation of d^2 with t was not a straight line relation.

The influence of natural convection on the burning process of droplets was studied by Kumagai and Isoda (15). A combustion

chamber that fell with a constant acceleration was used to produce a field with little or no gravitational acceleration. Combustion of fuel droplets in a freely falling chamber is not affected by natural convection and therefore the combustion process corresponded to that of a spherically symmetric combustion model. Burning rates of fuel droplets decreased as acceleration decreased and changed rapidly in the region of smaller values of acceleration. In the case of little or no acceleration, the experimental values of burning rate were about one half of the values calculated from the theory assuming steady state on a model of spherical symmetry.

An experimental study of the rate of evaporation of stationary droplets of water, methanol, cumene, pentane, and benzene was carried out by Hoffman and Gauvin (11). The investigation involved measurement of the evaporation rates of liquid droplets 0.4 to 1.4 millimeters in diameter suspended on thin glass fibers at the center of a heated stainless steel sphere. The gaseous environment consisted of the superheated vapor of the liquid under investigation. In all cases, the wall and gas temperatures were the same. The conclusion was that the evaporation rate was not governed by the rate of heat transfer by natural convection since no dependency of the Nusselt number on the Grashof number was found. On the other hand, the evaporation rates appeared to be satisfactorily predicted by the expression

$$\left[\left(\frac{dm}{dt}\right) (c_p) \,/\, (\pi d k_g) \right] (Pr)^{-1/3} = 3.2B^{0.97} \qquad (19)$$

over the range $0.03 < B < 1.0$.

None of the experimental work discussed so far has considered the case of uniform droplets moving freely under forced convection through a hot air stream. Preliminary work on this problem was done by Frazier and Hellier (7) and later by Bhogte (2) using a uniform stream of droplets generated by the induced breakup of a liquid jet from a fine capillary tube. Vaporization studies were conducted by directing the droplet stream horizontally through the center of an elevated temperature air jet. Both experiments confirmed the linear relationship between d^2 and t. However, vaporization rates obtained in both cases were significantly higher than similar data obtained by Ranz and Marshall and Hoffman and Gauvin using suspended droplets. These differences were postulated to be due to the use of freely moving droplets and higher temperatures than had been studied previously.

CHAPTER IV

EXPERIMENTAL APPARATUS AND PROCEDURE

The experiemental apparatus is a modification of equipment used by Bhogte (2) and consists of three major components:

1. Water storage and delivery system and droplet generating assembly;

2. Furnace and compressed air supply to deliver moving air at elevated temperatures;

3. Photographing assembly to record changing droplet diameters.

The water storage and delivery system and the furnace are shown schematically in Figure 1.

Water droplets of uniform size are produced by the breakup of a jet of water forced through a fine capillary tube. Breakup is induced by longitudinal vibrations in the capillary which are generated by a sonic driver. The droplet generating assembly is shown in Figure 2. A University Sound model ID-30 sonic driver having a frequency response range of 87-7500 Hz is driven by an Electronic Instrument Company model 377 audio generator and an Altec model 1570B amplifier. The signal from the audio generator is stabilized with a Sorenson and Company model 1000 A.C. voltage regulator. Between the sonic driver and the brass transmission chamber is a 0.002 inch thick copper diaphragm which transmits the vibrations from the sonic driver to the water in the chamber.

The cylindrical chamber measures two inches O.D. and tapers

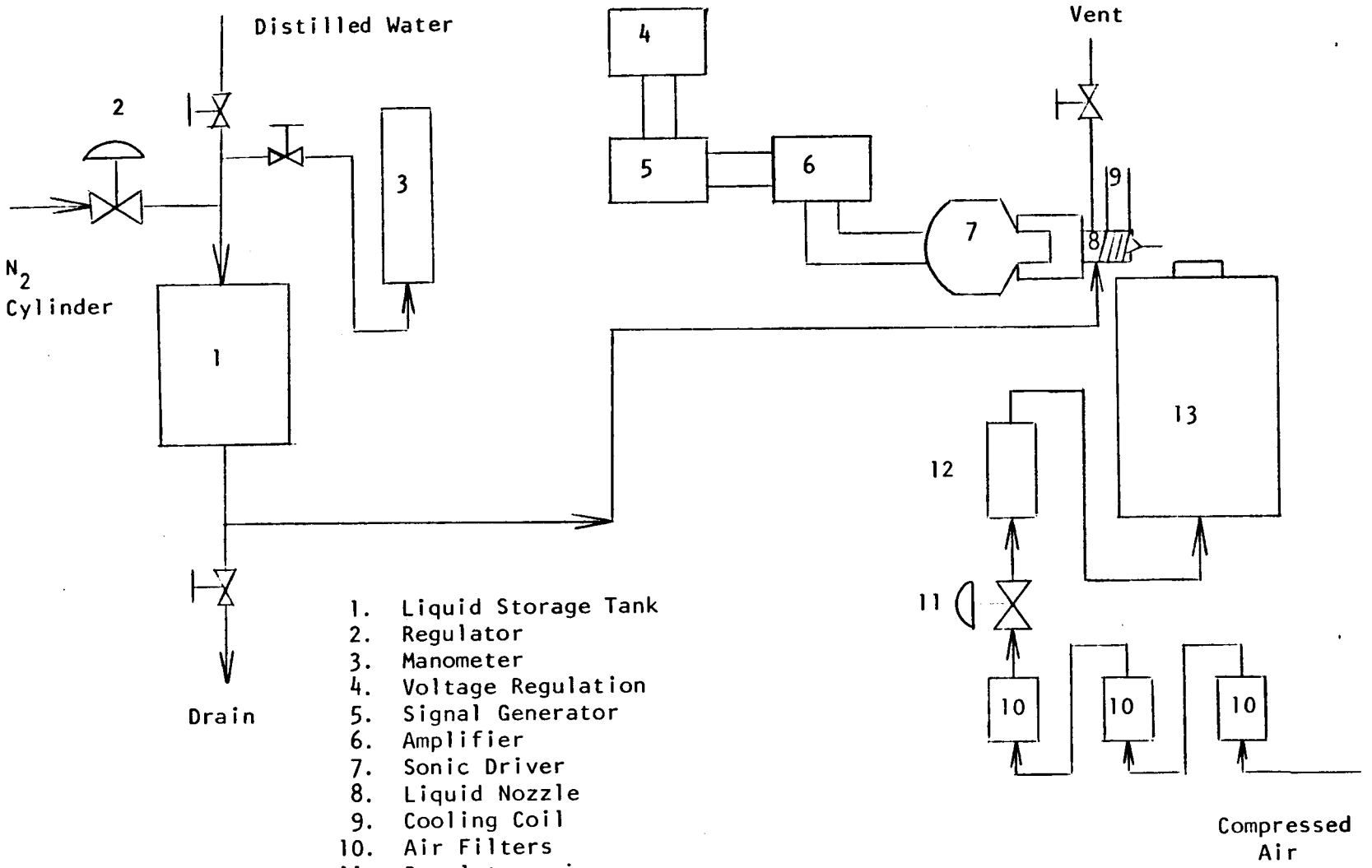

Figure 1. Experimental Setup

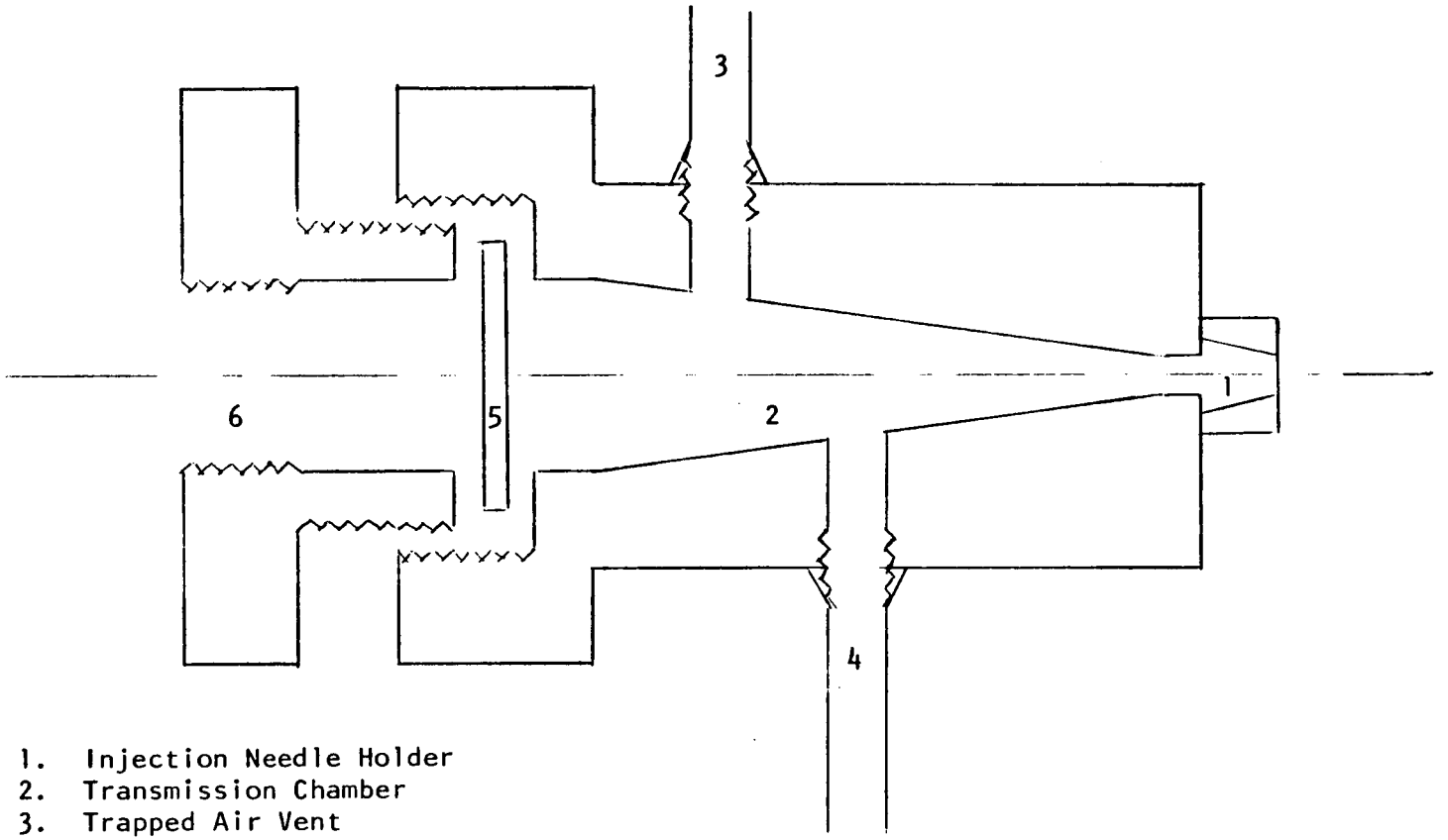

1. Injection Needle Holder
2. Transmission Chamber
3. Trapped Air Vent
4. Water Inlet
5. Copper Diaphragm
6. Sonic Driver Holder

Figure 2. Droplet Generating Assembly

inside from 3/4 inch to 1/4 inch over a length of 2 1/4 inches. At the outlet end of the transmission chamber, a standard injection needle holder is soldered. Stainless steel capillaries of varying diameters are soldered into standard injection needles; these are then fitted into the holder. Being able to change capillaries allows the study of droplets having different diameters. A coil of 1/8 inch copper tubing is soldered on the outside of the transmission chamber. Cooling water flows through the coil during a run to prevent the transmission chamber and the capillary from becoming hot. A vent valve at the top of the chamber allows the release of trapped air.

Distilled water is delivered to the transmission chamber from a nitrogen pressurized storage tank having a capicity of about 0.5 cubic feet. Pressure is regulated with a Honeywell regulator valve and is measured with a mercury manometer. Valves and drain lines are provided to purge and refill the tank as required. Sufficient pressure is applied to the tank to maintain a steady, horizontal stream of droplets with a trajectory which carries it beyond the edge of the furnace.

The water droplets are directed horizontally through a hot air stream near the exit of a vertically mounted tubular furnace. The furnace core consists of two alundum tubes, one with an inside diameter of 2 5/8 inches and the other with an outside diameter of 2 3/8 inches; the smaller one is mounted inside the larger one. Each tube has external grooves which are wound with 14 gauge Nichrome wire. Two seven Kva Variacs are used to control the current to each winding.

Housing for the entire core assembly consists of a rectangular

stainless steel shell measuring 12 inches wide by 12 inches deep by 18 inches high. Firebrick is used to insulate the core from the shell housing and blocks of transite are used at either end. The entire furnace assembly is mounted on a steel frame.

Compressed air at 120 psig. is used for the air stream through the furnace. The air passes through three filters:

1. Hannifin Crown Filter F-103;
2. A pressure vessel packed with filter paper;
3. Filter Manufacturing Company style number 6.

A Moore nullmatic valve model 41-30F is used to regulate the air flow. Air flow rate is measured with an inline rotameter, Brooks model 1111.

Air enters the furnace at the bottom, passes through the annulus between the two cylinders, and exits at the top. The inner core is packed with ceramic beads to increase the heat transfer between the tube surface and the center of the cylinder. The three inch space between the top of the inner core and the top of the outer core is also filled with beads which are smaller in size. Above the surface of the furnace is a one inch thick piece of firebrick with a 2 1/2 inch diameter hole cut through it. Three 100 mesh nickel screens separated by nickel rings are placed inside the firebrick normal to the air flow to insure a flat velocity profile in the exiting hot air stream.

Air temperature is measured with a one mil platinum and platinum-10 percent rhodium thermocouple which is mounted on a three-way sliding support stand attached to the furnace support frame. Three-way movement allows the thermocouple junction to be placed directly in the plane of

the moving droplets and moved to any position in order to measure temperature profiles in the hot air zone. Thermocouple potential difference is measured with a Leeds-Northrup potentiometer using an ice bath as the reference junction.

A Graphic View camera is used to provide a photographic record of the change in droplet diameter. It is mounted on a sliding stand which allows movement in two directions. Lateral motion of the camera is read on a scale attached to the stand. The Kodak Plus-X film is illuminated by a single flash of a Strobotac which is placed behind the droplet stream. Droplet frequency is also measured with the Strobotac. A series of microscope lenses replaces the standard camera lens so that variable magnification can be achieved.

Three basic steps comprise the experimental procedure for determining the mass rate of change of the vaporizing droplets:

1. Establish a coordinate system with the droplet stream, a stainless steel wire, the thermocouple junction, and the camera;

2. Establish a steady state temperature in the air stream and a steady stream of uniform droplets;

3. Photograph the droplets at intervals in the hot air stream and measure the temperature at each point.

At the start of each experimental run, the trajectory of the droplet stream is determined. Then a five mil stainless steel wire is mounted in the plane of the trajectory such that the droplets and the wire will both be on each photographic plate. The camera is positioned so that the wire and the droplets remain in focus as the camera moves laterally across the diameter of the furnace opening. Finally

the thermocouple is positioned so that the junction is at the same level as the droplet stream.

Air flow through the furnace is set at a level high enough to insure a flat temperature profile but low enough not to blow the droplets out of their trajectory. Current to the heating coils is increased in stages until the desired temperature is maintained without change. At this point the region of flattest temperature profile can be determined; this region is then used as the evaporating zone for the droplets. Preliminary work has shown that the maximum distance of constant temperature is about 30 millimeters so all photographs are taken in this region.

A uniform stream of droplets is then introduced into the hot air stream. This is done by pressurizing the storage tank and allowing the jet of water from the capillary to stabilize. Any air trapped in the transmission chamber is purged through a valve located at the top of the chamber. When the water jet is stable, the audio generator is adjusted to a frequency which generated droplets of uniform size and velocity. Frequencies between 2500 and 3500 Hz produce the most stable droplet streams.

Photographs of the droplets and the wire are then taken at intervals along the trajectory of the stream. At each point the frequency of the droplets is determined by stopping the motion with the stroboscope and recording the frequency at which the motion is stopped. Droplet motion is stopped photographically by opening the camera shutter for a single flash of the stroboscope. The location of each photograph is noted from the scale reading taken as the camera moves horizontally; this scale can be read to the nearest millimeter.

After a series of photographs has been made, the temperature profile across the trajectory is measured. The thermocouple bead is positioned so that it is in focus on the ground glass plate in the camera at each location where a photograph is made. This method insures that the temperature is measured at the exact location of each photograph.

The final step in an experimental run is to develop the plates and analyze the results. A four-step developing procedure is used which starts with Microdol-X developer. After drying, the negatives are marked with an identifying run number and position number. Depending on the initial droplet diameter and the magnification, anywhere between eight and 14 droplets will apear on a given plate. The center of the plate appears at the intersection of two cross hairs which are present in one of the lenses attached to the camera.

CHAPTER V

RESULTS AND INTERPRETATION

Six experimental runs at different temperatures with a 0.012 inch O.D. capillary were made. Four of the six runs consisted of a series of 12 photographs with two photographs taken at each of six locations in the hot air field. The other two runs each consisted of a series of ten photographs with each one taken at a different location.

Thermocouple temperature measurements were corrected for the effects of radiant heat transfer from the thermocouple junction. The junction was considered to be a spherical bead having a measured diameter of 0.0050 centimeters formed by the weld between the two one mil thermocouple wires. Net heat radiated from the bead, neglecting heat radiated from the screens, is given by

$$q_r = \varepsilon \sigma T_c^4 \tag{20}$$

where ε is the emissivity of the bead and has a value of 0.15 for platinum at the temperatures considered here (21). Heat conduction from the air stream to the center of the bead is given by

$$q_s = h(T_\infty - T_c) \simeq \frac{2k_a}{d_o} (T_\infty - T_c) \tag{21}$$

since $Nu = hd_o/k_a \simeq 2.0$ for the case of a stationary bead in a moving air stream for small values of Re. At the surface of the bead, $q_r = q_s$ and Equations (20) and (21) can be rewritten as

$$T_\infty = T_c + \frac{d_o \varepsilon \sigma}{k_a} T_c^4 \qquad (22)$$

where k_a is the thermal conductivity of the air at temperature T_c evaluated from (5)

$$k_a = 76.2 \times 10^{-6} \left(\frac{T_c}{T_b}\right)^{0.766} \text{ cal/sec-cm-}^{o}\text{K.} \qquad (23)$$

Table 2 shows the results of the calculations. Although the temperature corrections were small (less than 0.5 percent), the calculated values of T_∞ were used throughout the remainder of the data analysis.

Droplet diameters were measured from the photographic negatives using a Leeds-Northrup Microdensitometer. The densitometer light filament was passed over the droplet image in a direction perpendicular to its line of flight at its widest diameter. Approximately six droplets at the center of each plate were used. Traces of the wire image which establishes the magnification for each plate were made at three points which corresponded roughly to the locations of the two droplets farthest from the center of the plate and the one droplet closest to the center. A typical photograph is shown in Figure 3, and the densitometer trace of one of the droplets on the same plate is shown in Figure 4. A trace of the wire image on the same plate is shown in Appendix B in order to indicate the sharpness of the edges of a trace of a solid object.

Actual droplet diameter was calculated from the diameter of the densitometer trace. Trace diameter was measured at the widest point

TABLE 2

EXPERIMENTAL RESULTS

Run	T_c, °C	T_∞, °C	Residence Time in Hot Air Zone Prior to Start of Data		Mean Droplet Spacing cm	d_o, cm	$\dot{m} \times 10^6$, gm/sec	Velocities, cm/sec		
			Time Msec	Distance mm				v_a	v_d	v_∞
121174	863	868	9.7	23.7	.0937	.0291	133.6	99.3	244.2	263.6
4175	784	788	9.2	15.7	.0715	.0287	55.0	44.4	170.9	176.5
6675	681	684	8.6	17.7	.0626	.0270	90.2	66.6	207.2	217.7
62075	732	735	9.5	22.2	.0692	.0291	150.3	75.8	233.8	245.8
62175	694	697	9.7	27.7	.0861	.0296	97.9	75.8	284.8	294.7
62475	788	792	7.8	17.7	.0681	.0266	173.8	75.1	225.8	238.0

Run 62075

Plate 3

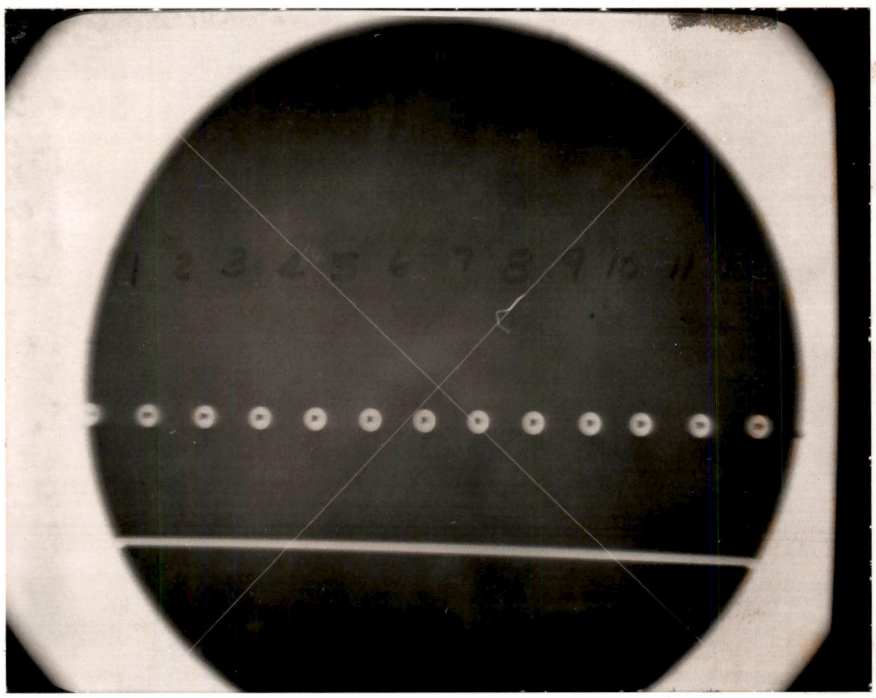

Figure 3. Photograph of a Typical Plate

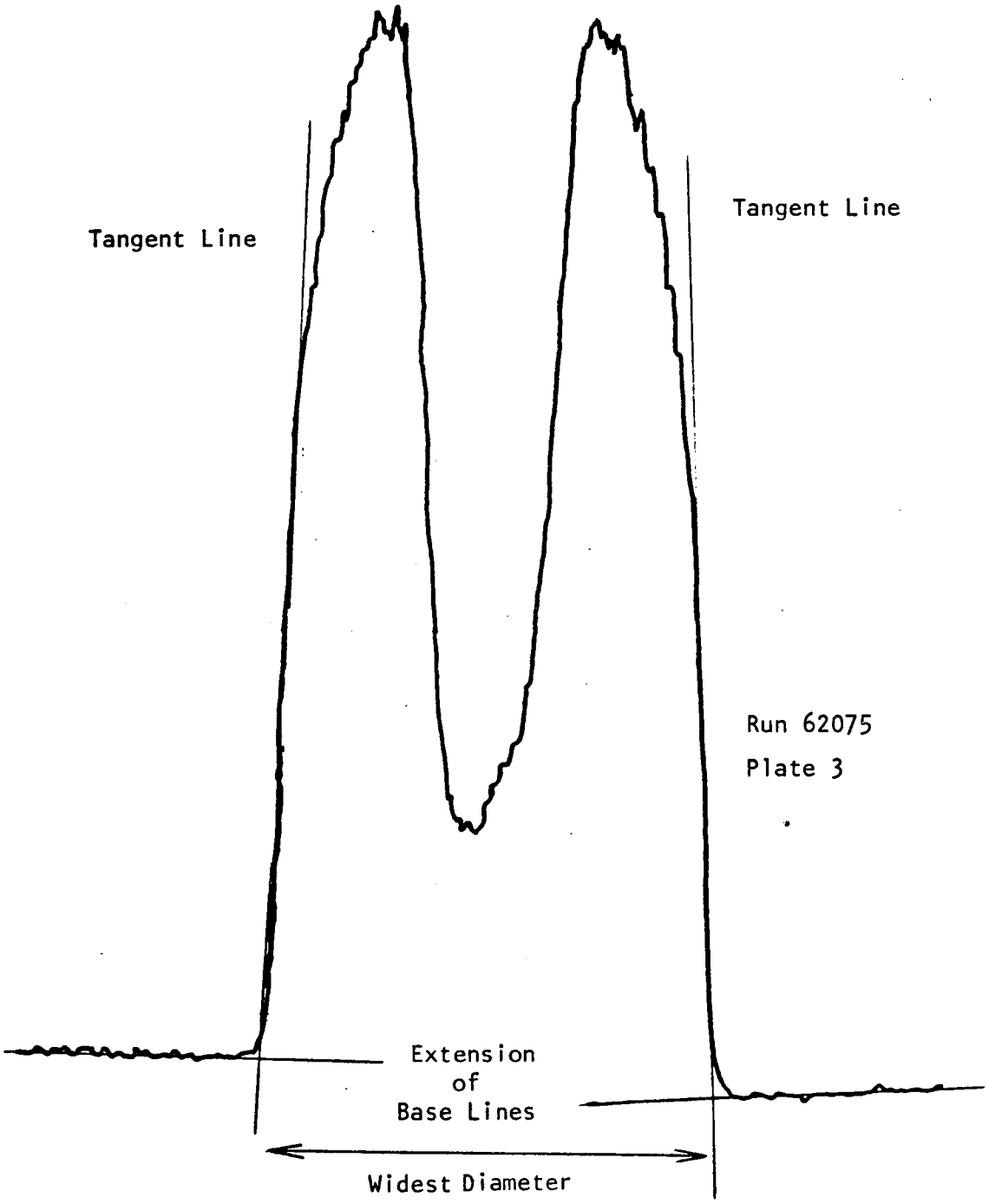

Figure 4. Microdensitometer Trace of a Single Droplet

which was at the intersection of lines drawn tangent to the edge of the trace and the extension of the base lines; these construction lines are shown in Figure 4. Traces of the wire were treated in the same manner as traces of the droplets. The ratio of the diameter of the trace of the wire image to the diameter of the wire as measured under a microscope was used as a magnification factor to calculate the diameter of the droplet from the diameter of its densitometer trace. The magnification factor for converting from densitometer trace diameters to actual diameters varied, depending on the location of the camera lenses relative to the droplet stream, from 272 for runs with approximately 14 droplets per plate to 454 for runs with approximately eight droplets per plate.

Wire diameter was measured at approximately each of the locations where a photograph was made and an average of all the measurements was used in the calculations. The nominal wire diameter was 120 microns and the average range of measurements for the six runs was $\pm$ 3.8 percent. The average wire trace diameter from all plates in a given run was used with the average measured wire diameter to calculate the actual droplet diameter.

The densitometer was also used to determine the distance from the forward edge of each droplet to the center of each plate. The center of the first plate was considered the starting point of each run. Total distance of each droplet from the start was calculated from the distance as measured by the scale attached to the camera mount. Droplet spacing was then the difference in total distance between two adjacent droplets. It was observed that the droplet spacing

decreased as the total distance increased due to the decrease in droplet velocity as the diameter decreased. A typical plot of droplet spacing as a function of total distance is shown in Figure 5; similar plots for the other five runs are shown in Appendix C. The least squares line drawn through the data was used to calculate the droplet spacing for each droplet. The frequency of the droplets as measured by the stroboscope was used with the measured total distance of travel and the distance between droplets to calculate the total time of flight of each droplet from the starting point. These frequencies plus additional experimental data are tabulated in Appendix D.

Since steady state vaporization cannot occur until the droplet reaches a uniform temperature, an estimate was made of the time required after its introduction into the hot air stream for the droplet to reach 90 percent of its boiling temperature at a distance $r/r_o = 0.4$ into the droplet. This estimate was used to establish the proper starting location for the determination of t_o and d_o. One-dimensional heat flow in a stationary sphere, constant physical properties, an initial condition of uniform temperature throughout the droplet, and heat input by convection at the surface was the model used in the calculation. A preliminary estimate of the initial droplet diameter was required and was determined from the intercept of a linear least squares fit of d^2 as a function of t.

An estimate of the overall surface heat transfer coefficient was also required. A conservative estimate was made using Ranz and Marshall's correlation:

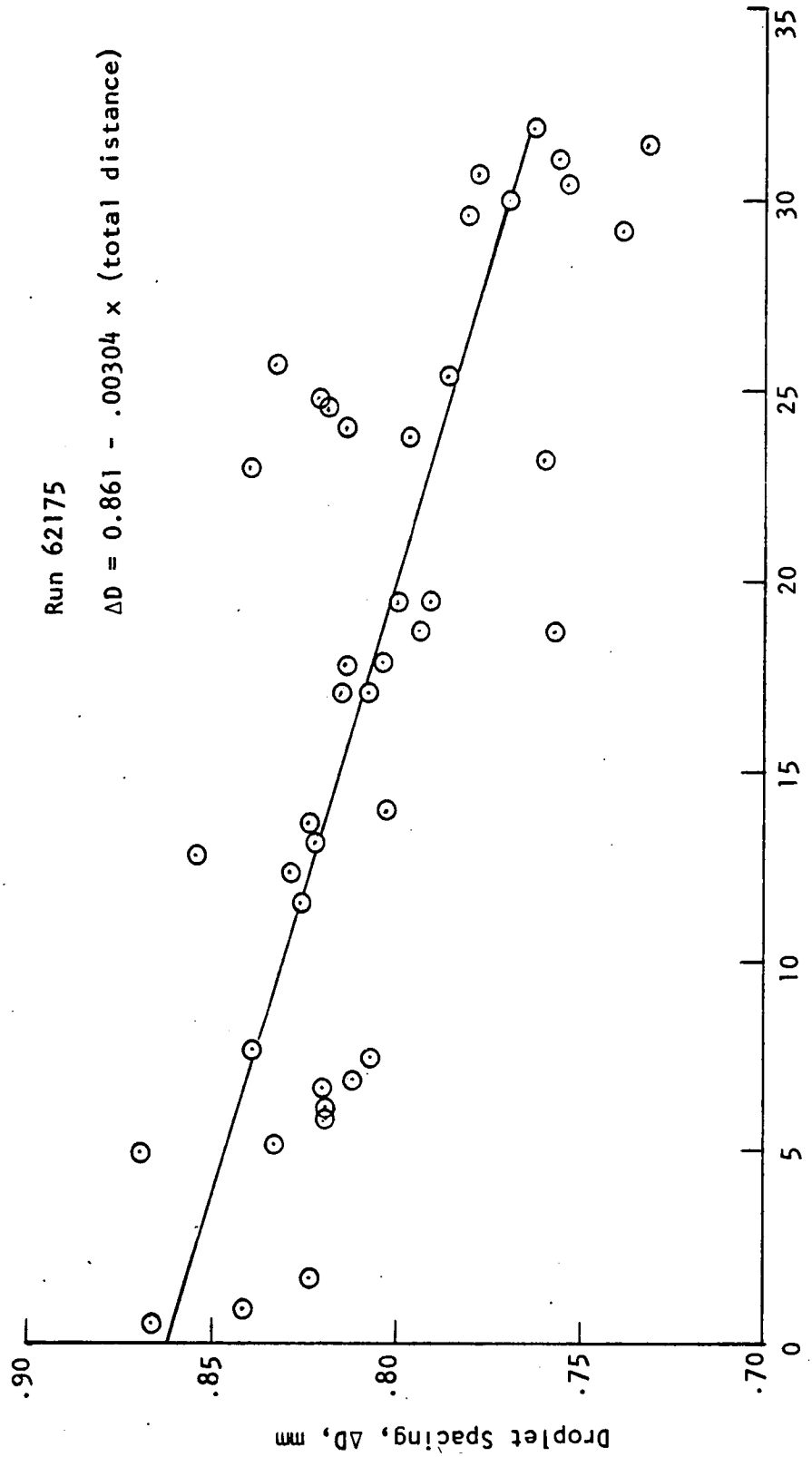

Figure 5. Droplet Spacing for a Typical Run

$$Nu = \frac{hd_o}{k_a} = 2.0 + 0.60\ Re^{1/2}\ Pr^{1/3} \qquad (8)$$

This was considered a conservative estimate because their correlation was based on the vaporization of suspended droplets in a moving hot air stream and previous work (2, 7) has shown that the vaporization rate is higher for the case of forced convection of droplets in a moving hot air stream. Therefore the overall heat transfer coefficient should be greater for the present case than for the case of stationary droplets.

The appropriate heat transfer equations have been solved numerically by Schneider (18) and are presented in chart form. Dimensionless temperature $(T - T_o)/(T_\infty - T_o)$ as a function of $\frac{k_a}{\rho_\ell c_p} \frac{t}{r_o^2}$ with Biot number ($Bi = \frac{hr_o}{k_a} = \frac{hd_o}{2k_a} = \frac{1}{2} Nu$) as a parameter is plotted for given values of r/r_o ranging from $r/r_o = 0$ (at the center of the droplet) to $r/r_o = 1$ (at the surface of the droplet). A value of $r/r_o = 0.4$ was selected for this analysis since preliminary work had shown that at the highest temperatures studied, the diameters of the droplets did not decrease by more than about 20 percent. The results of these calculations are shown in Table 2. Residence time prior to steady state vaporization is defined as the time required for the droplet to reach 90 percent of its boiling temperature at a point where $r/r_o = 0.4$ after being introduced into a constant temperature medium.

Next it was determined where the beginning of the hot air zone was located in relation to the first plate made for each run. A typical temperature profile showing the edge of the furnace and the location of the first plate is shown in Figure 6. Temperature profiles for the other five runs are shown in Appendix E. For the remainder of the

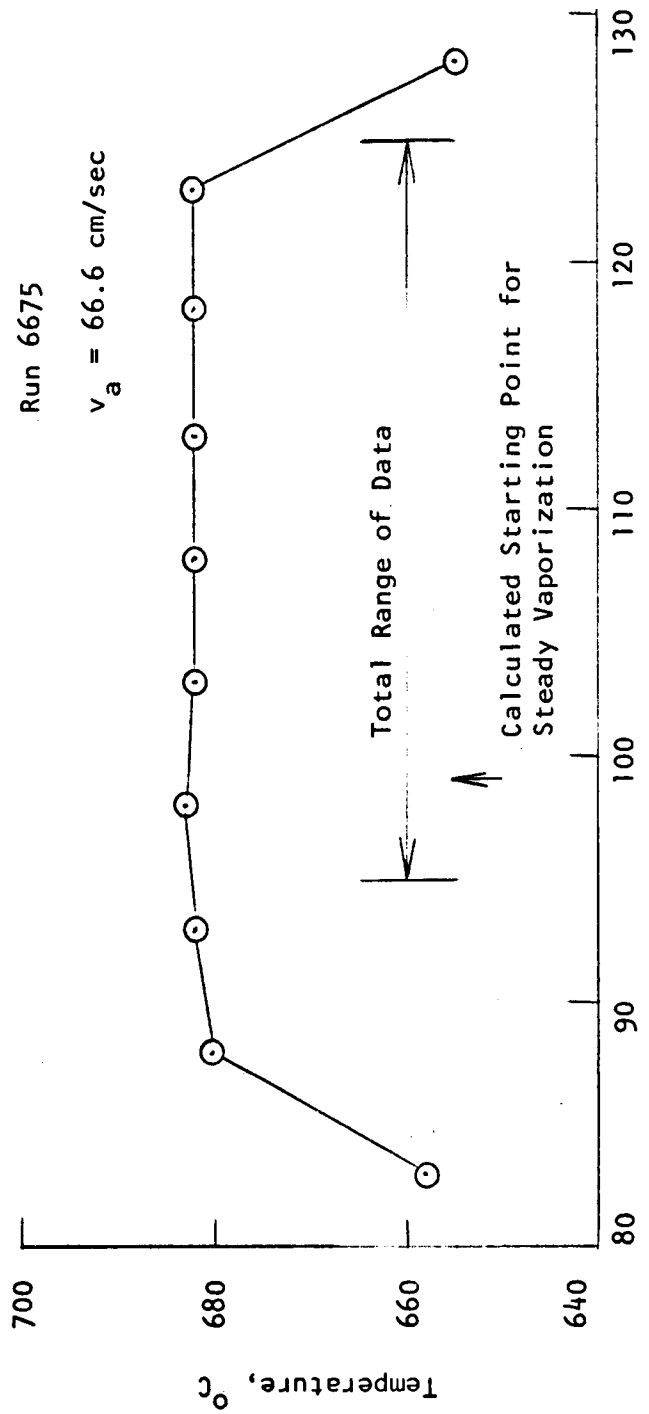

Figure 6. Typical Temperature Profile

calculations, only those plates taken at locations beyond the calculated residence time for steady vaporization were considered.

The final plot for each run consisted of values of d^2 plotted as a function of t. These plots are shown in Figures 7a-f. Vaporization rates were calculated from Equation (6) using the slope of the least squares line for each set of data. Initial droplet diameter was taken as the diameter at time equal to the minimum residence time for steady evaporation. These data are summarized in Table 2. Since the final values of d_o agreed to within 1.5 percent of the values used to calculate minimum residence times, no further refinements to those calculations were made.

Vaporization rates that would occur in an identical medium but under conditions of no motion relative to the droplet ($\dot{m}_o$) were calculated as described by Frazier and Chang (6). Corrected ambient gas temperatures and experimental values of d_o were used as inputs to a computer program to calculate $\dot{m}_o$ for conditions of no radiant heat flux absorbed by the droplet ($q_s^r = 0$) and for the case which does consider radiant heat flux ($q_s^r \neq 0$). For the latter case, the view factor was taken as 0.22 as suggested by Crosby and Stewart (4) in an analysis of work reported by Frazier and Hellier (7). Calculated values of $\dot{m}_o$ for the cases with and without radiation are shown in Table 3 along with the calculated droplet surface temperature, T_s. Since the differences in $\dot{m}_o$ calculated for the cases both with and without radiation are small (about 5.2 percent), no attempt was made to further refine the value of the view factor to be used.

One purpose of the experiment was to determine the effect of

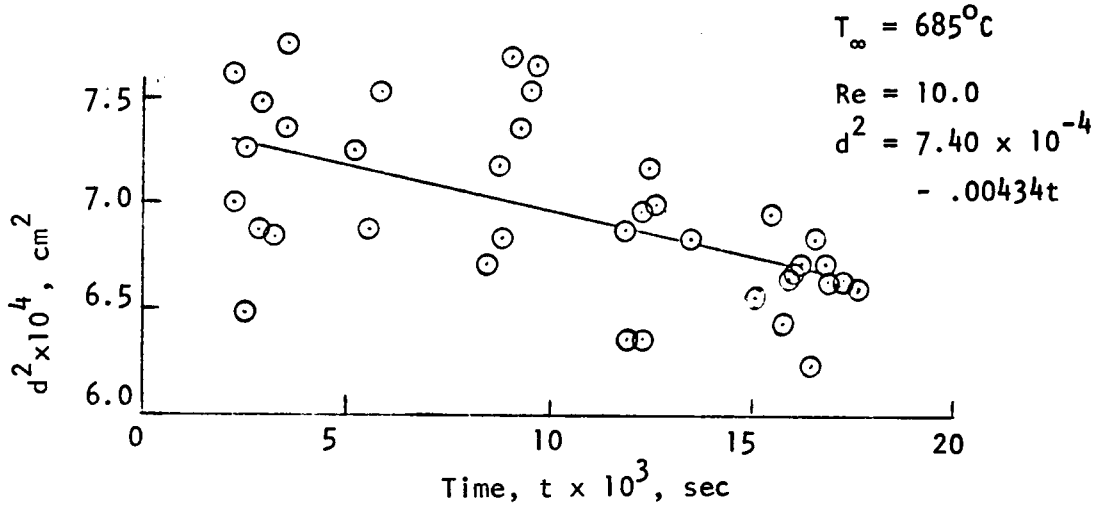

Figure 7c. Run 6675

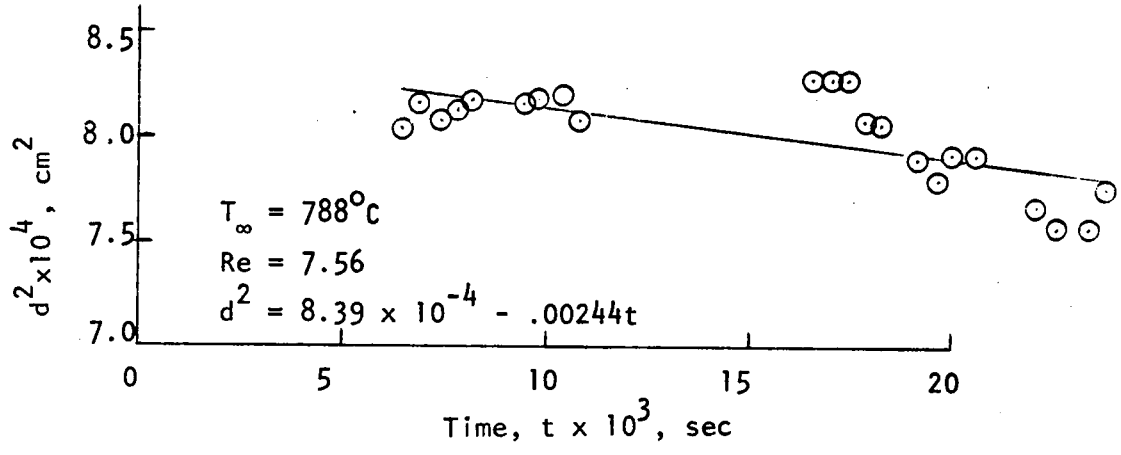

Figure 7b. Run 4175

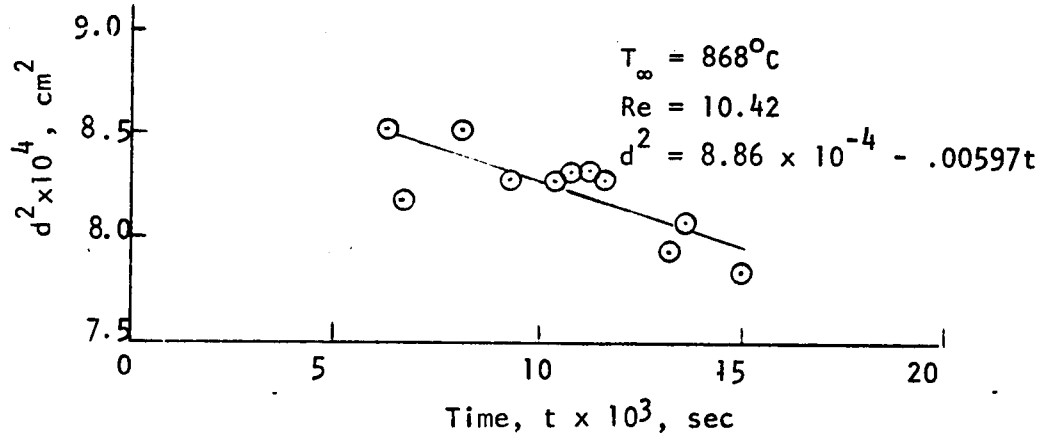

Figure 7a. Run 121174

Figure 7. Variation of d^2 with Time

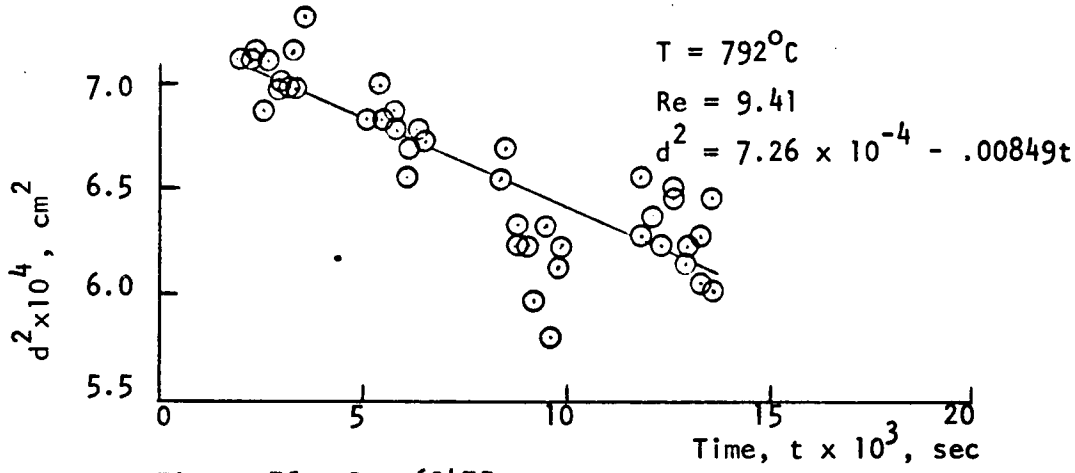

Figure 7f. Run 62475

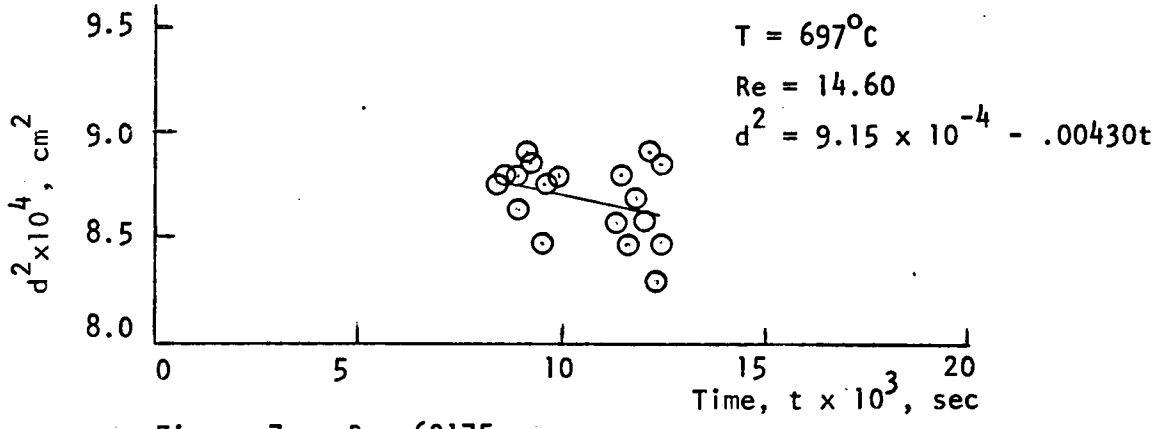

Figure 7e. Run 62175

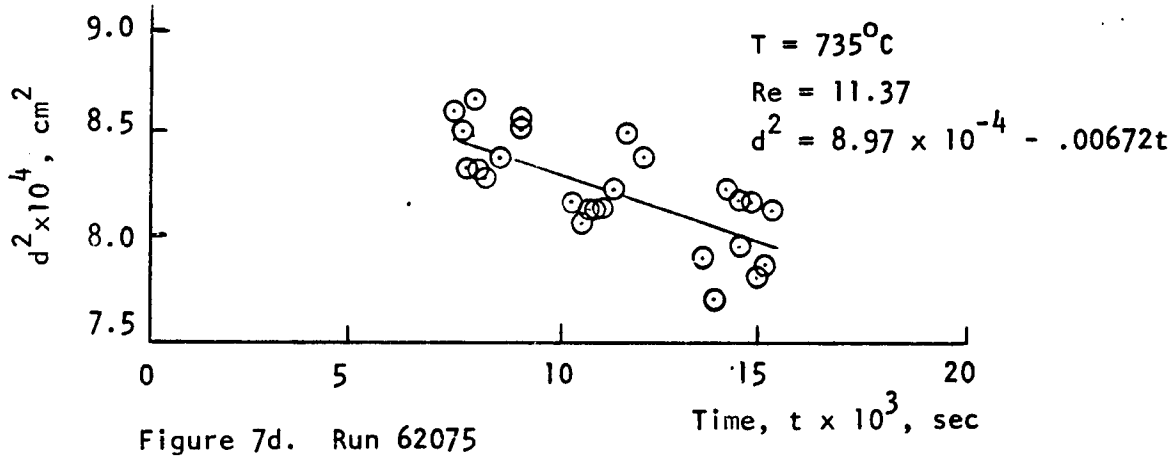

Figure 7d. Run 62075

Figure 7. (continued)

TABLE 3

CALCULATED RESULTS

Run	$\dot{m}_o \times 10^6$, gm/sec With Radiation	$\dot{m}_o \times 10^6$, gm/sec Without Radiation	T_s, ^oC	Re	$\dot{m}/\dot{m}_o$	Pr	Gr	0.30 $Gr^{1/2}Pr^{1/3}$	We
121174	28.3	26.4	70	10.42	4.72	.727	.0480	.0591	.00760
4175	24.4	23.0	69	7.56	2.26	.730	.0528	.0621	.00354
6675	18.8	18.1	66	10.02	4.78	.733	.0536	.0626	.00542
62075	22.5	21.4	69	11.37	6.68	.731	.0603	.0664	.00723
62175	21.3	20.3	68	14.60	4.60	.732	.0685	.0708	.01085
62475	22.7	21.5	69	9.41	7.65	.730	.0420	.0554	.00595

forced convection on the droplet vaporization rate. Because of the limited range of the experimental data, only the dependence on Re was considered and an equation of the form

$$\dot{m} = \dot{m}_o (1 + a\ Re^n) \tag{24}$$

was proposed. Rearranging Equation (24) resulted in the form

$$\frac{\dot{m}}{m_o} - 1 = a\ Re^n \tag{25}$$

which could readily be plotted in log-log form to determine the constants a and n (see Figure 8).

Physical properties used to calculate the droplet Re and other non-dimensional parameters to be discussed later were evaluated at the mean temperature between the droplet surface temperature, T_s, and the free stream air temperature, T_∞. Although the film surrounding the droplet was a mixture of water vapor and air, the maximum mole fraction of water vapor in air would be about 0.3 for a droplet in a stagnant medium at the same experimental free stream temperature. The actual mole fraction for this experiment was probably considerably less than 0.3, and thus the effect of the presence of water vapor on the physical properties of air was neglected. Droplet velocity was taken as the resultant of the air stream velocity in a vertical direction and the droplet velocity in a horizontal direction; these velocities are summarized in Table 2, page 31. Values of several of the calculated non-dimensional parameters are summarized in Table 3.

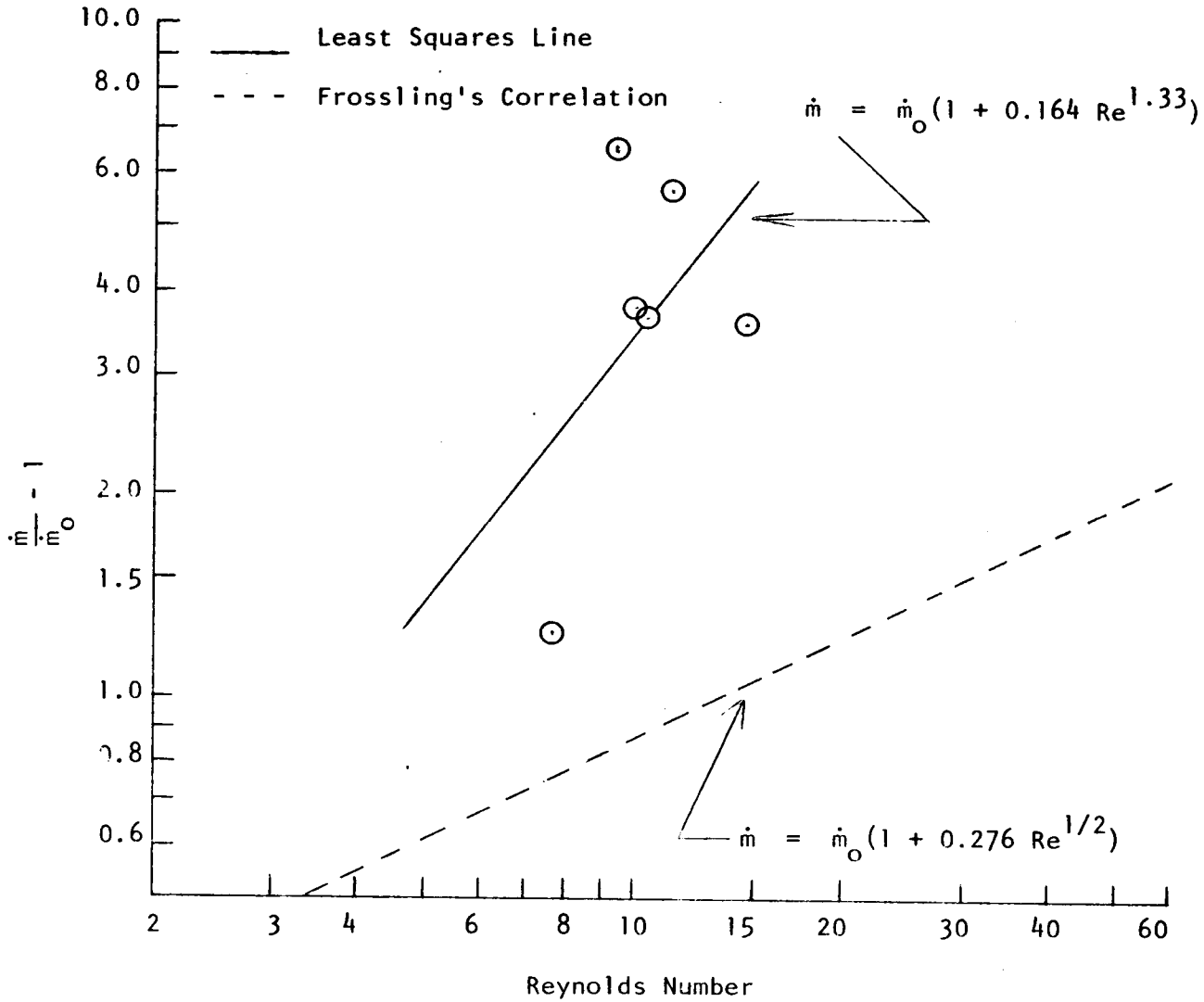

Figure 8. Droplet Reynolds Number Dependence of Vaporization Rate

A linear least squares fit of the data plotted in Figure 8 resulted in the equation

$$\dot{m} = \dot{m}_o (1 + 0.164\ Re^{1.33}). \tag{26}$$

Although the correlation obtained was not statistically significant, it did suggest that forced convection exerted a much greater effect on vaporization rate than had previously been reported (1, 8, 13, 17, 20). This is especially apparent when one considers the vaporization rates which would be predicted from correlations such as Frossling's which is also plotted in Figure 8.

In an attempt to determine factors other than forced convection which may have influenced the vaporization rates, three possible interactions were studied:

1. Possible effects of natural convection correlated in terms of the Grashof number, Gr;

2. Possibility that the Reynolds number of the flow field was small enough that surface tension and viscous forces were significant;

3. Possibility that the distance between the droplets was small enough that the droplets were interacting with each other, i.e., a "wake effect."

According to Yuge (25), the effect of natural convection may be expressed in the form

$$Nu = 2.0 + 0(Gr^{0.5}) \tag{27}$$

for $Gr \ll 1$ where 0 indicates order of magnitude. An extrapolation of

his data to small values of Gr of a plot shown in the reference suggests a coefficient ≃ 0.3. Also, since work by several authors (8, 11, 17) has indicated a dependence of vaporization rate on $Pr^{1/3}$, the equation

$$\dot{m} = \dot{m}_o (1 + a\, Re^n + 0.30\, Gr^{1/2}\, Pr^{1/3}) \qquad (28)$$

was considered. Equation (28) was rearranged in the same manner as Equation (24) and a log-log plot yielded values for the parameters a and n. Calculation of Gr and Pr was based on the mean film temperature as discussed earlier; the results appear in Table 3. The numerical values of the function $0.30\, Gr^{1/2}\, Pr^{1/3}$ ranged from 0.0554 to 0.0708 which are small compared with the remaining terms in Equation (28). The linear least squares evaluation of a and n resulted in the values n = 1.36 and a = 0.150; again, the scatter in the data was such that the correlation was not statistically significant. Since the inclusion of a term accounting for natural convection had no significant effect on the previously determined Re correlation, it was concluded that natural convection was a negligible effect and did not account for either the scatter in the data or the difference in vaporization rates obtained in this work and those obtained in previous experiments.

The second possibility is that the shear of the droplet by the flow field was sufficient to cause oscillations and deformation of the droplets. According to Sevik and Park (19), several forces can act on a droplet to cause this distortion:

1. A droplet elongates into the shape of a prolate ellipsoid of revolution under the action of viscous shear. - Elongated droplets

were noticed in some cases as can be seen in Figure 9; this suggests that oscillation of droplets was occurring tc some extent.

2. The deformation is determined by a Weber number, We, given by

$$We = \frac{\rho v_\infty^2}{\sigma_d / r_o} \tag{29}$$

3. Breakup of the droplet occurs at a critical value of the Weber number which depends on the flow field and is approximately equal to 1.0 for the case of a water droplet in an air stream. The values of We calculated for this experiment ranged from 0.00354 to 0.01085, however, which are well below the critical value for droplet breakup to occur.

Oscillations still could have influenced the vaporization rates, however, and so an equation of the form

$$\dot{m} = \dot{m}_o (1 + a\ Re^n + b\ We^m) \tag{30}$$

was postulated to account for the difference in f(Re) between this work and previous experiments. Frossling's form of $a\ Re^n = 0.276\ Re^{1/2}$ was assumed and the constants b and m determined; these had values of $m = 1.38$ and $b = 7.93$. The correlation was not statistically significant, however, and only suggests that shear forces acting on the droplet may be significant.

A third possible effect was that the distance between droplets

Run 4175

Plate 2

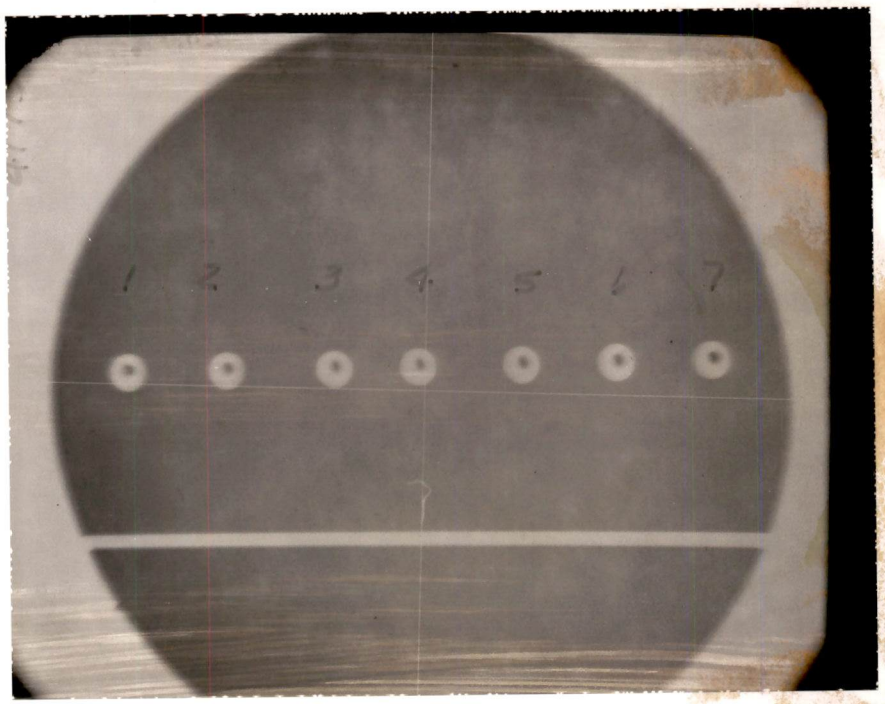

Figure 9. Photograph of a Plate Showing Slightly Elongated Droplets

was small enough that the vaporization of a droplet could be influenced by the presence of a "wake effect" from the droplet preceding it. The effect of the wake would be to increase the mole fraction of water vapor in the vicinity of the following droplet and thus decrease the vaporization rate. Quantitatively, the effect should be a function of both the distance between the droplets and the angle of v_∞ which is the resultant of the droplet velocity v_d in a horizontal direction and the air velocity v_a in a vertical direction. It was postulated that this droplet interaction effect might take the form

$$\gamma = \exp\left[- \frac{c'\Delta D}{d_o} \left(1 + \cos\left(90 - \delta\right)\right)\right] \tag{31}$$

where δ is the angle of the resultant velocity v_∞ from the horizontal, ΔD is the spacing between droplets, and c' is a constant. This form seems to behave properly qualitatively in the limits as $\Delta D \to 0 (v_a = 0)$ and $\delta \to 90 (v_d = 0)$. However, the effect on $\dot{m}$ should be negative, and if this effect were significant in this particular experiment, it must be evaluated in conjunction with another effect, for example, We, to explain the scatter in the data and the differences in results between this work and previous work. A possible correlation then might be of the form

$$\dot{m} = \dot{m}_o \left(1 + a\, Re^n + We^m - c\gamma\right). \tag{31}$$

Because of the limited amount of experimental data available in this work, however, one is unable to make statistically significant estimates of these parameters.

CHAPTER VI

CONCLUSIONS AND RECOMMENDATIONS

Although the data obtained in this work were taken over a limited range of droplet Reynolds number (7.6-14.6) and temperature (684-868°C) and showed significant scatter, the results show that the vaporization rates of freely moving droplets are greater than the vaporization rates of droplets suspended in a hot air stream. In particular, the vaporization rate-Reynolds number correlation obtained here,

$$\dot{m} = \dot{m}_o \left(1 + 0.164 \, Re^{1.33} \right) \qquad (26)$$

predicts significantly higher vaporization rates than Frossling's correlation

$$\dot{m} = \dot{m}_o \left(1 + 0.276 \, Re^{1/2} \right) \qquad (7)$$

which was based on stationary suspended droplets in a moving air field.

Attempts were made to determine whether effects other than forced convection enhanced the vaporization rates. Two factors which were considered are discussed below:

1. Natural convection does not appear to be a strong influence in increasing the vaporization rates in these experiments. Natural

convection effects calculated according to existing correlations ranged from 5.5 to 7.1 percent of the experimental vaporization rates and had no significant effect on the experimentally determined Reynolds number correlation.

2. There is a possibility that at low Reynolds numbers, the shear of the droplet by the flow field was sufficient to cause oscillations of the droplets. These oscillations would tend to enhance vaporization rates by disturbing the vapor film in the vicinity of the droplets. This effect should be characterized in terms of the Weber number; however, an attempt to correlate the data to account for this effect was not statistically significant.

Another factor which could have been partly responsible for the scatter in the data was also considered. Interactions between droplets could be significant if the vertical air stream velocity and/or the distance between droplets are small enough that the mole fraction of water vapor in the film adjacent to a droplet is increased by the wake of the droplet preceeding it. This effect would tend to lower the vaporization rates. Again, however, the data presented here are not sufficient to establish this interaction effect.

Although the data presented in this work show a significant amount of scatter, the experimental method appears to be valid for studying the effects of forced convection on droplets on the order of a few hundred microns in size. Several recommendations for refinements in experimental apparatus and technique and for future work are presented below:

1. The range of Reynolds number which can be studied is

primarily determined by the size of the capillary which determines the size of the droplets. This range should be increased by extension of the work to smaller sized capillaries.

2. A larger diameter hot air zone would permit longer residence time of the droplets in the vaporizing region. This would increase the degree of vaporization which occurs and the amount of data which can be taken and possibly decrease the scatter.

3. Another way to increase the degree of vaporization is to increase the temperature beyond those that were studied here.

4. A problem associated with the design of the furnace used in these experiments was the accurate evaluation of radiant heat transfer effects from the core of the furnace and the screens used at the furnace opening. The use of an optical pyrometer for temperature measurements might be feasible at higher temperature levels.

5. A better coordinate positioning device should be designed so that the positions of the camera, thermocouple junction, nozzle, and edge of the furnace opening can all be determined simultaneously using the same scale.

6. The air stream was assumed to have a uniform velocity profile across the furnace opening; this could easily be verified by hot wire measurements.

7. Effects of relative humidity of the air stream were considered negligible in this experiment. The relative humidity of the air stream should be measured or the air should be dried before it passes through the furnace to insure that this effect is negligible.

8. This experimental method could be extended to other

noncombustible and combustible liquids by enclosing the area above the furnace opening with a suitable shield and providing glass or quartz windows for the camera and stroboscope light.

LIST OF REFERENCES

LIST OF REFERENCES

1. Agoston, G. A., H. Wise, and W. A. Rosser, Sixth International Symposium on Combustion, Rheinhold Publishing Corporation, New York (1957), pp. 708-717.

2. Bhogte, S. M., M. S. Thesis, The University of Tennessee, Knoxville, 1972.

3. Bolt, J. A. and M. A. Saad, Sixth International Symposium on Combustion, Rheinhold Publishing Corporation, New York (1957), pp. 717-726.

4. Crosby, E. A. and W. E. Stewart, I&EC Fund., 9, 3, 515-517 (1970).

5. Eckert, E. R. G. and R. M. Drake, Jr., Heat and Mass Transfer, McGraw-Hill Book Company, Inc., 1959.

6. Frazier, G. C., Jr. and H. W. Chang, unpublished paper (1975).

7. Frazier, G. C., Jr. and W. W. Hellier, Jr., I&EC Fund., 8, 4, 807-810 (1969).

8. Frossling, N., Gerlands Beitr. Geophys., 52, 170 (1938).

9. Godsave, G. A. E., Fourth International Symposium on Combustion, Williams and Wilkins Company, Baltimore (1953), pp. 818-829.

10. Hall, A. R. and J. Diederichsen, Fourth International Symposium on Combustion, Williams and Wilkins Company, Baltimore (1953), pp. 837-846.

11. Hoffman, T. W. and W. H. Gauvin, Canadian Journal of Chemical Engineering, 38, 129-137 (1960).

12. Hottel, H. C., G. C. Williams and H. C. Simpson, Fifth International Symposium on Combustion. Rheinhold Publishing Corporation, New York (1955), pp. 101-129.

13. Ingebo, R. D., Sixth International Symposium on Combustion. Rheinhold Publishing Corporation, New York (1955), pp. 684-687.

14. Kobayasi, K., Trans. J. S. M. E., 20, 826-831 (1954).

15. Kumagai, S., and H. Isoda, Sixth International Symposium on

Combustion, Rheinhold Publishing Corporation, New York (1957), pp. 726-732.

16. Nishiwaki, N., Fifth International Symposium on Combustion, Rheinhold Publishing Corporation, New York (1955), pp. 148-158.

17. Ranz, W. E. and W. R. Marshall, Chem. Eng. Prog., 48, 141, 173 (1952).

18. Schneider, P. J., Temperature Response Charts, New York: John Wiley and Sons, Inc., 1963.

19. Sevik, M. and S. H. Park, J. of Fluids Engineering, 95, 53-60 (1973).

20. Spalding, D. B., Fourth International Symposium on Combustion, Williams and Wilkins Company, Baltimore (1953), pp. 847-864.

21. Wiebelt, J. A., Engineering Radiation Heat Transfer, New York: Holt Rinehard and Winston, 1965.

22. Williams, A., Combustion and Flame, 21, 1-31 (1973).

23. Williams, F. A., Combustion Theory, Addison-Wesley Publishing Company, Inc., Reading, Massachusetts, 1965.

24. Wise, H., J. Lorrell, and B. J. Wood, Fifth International Symposium on Combustion, Rheinhold Publishing Corporation, New York (1955), pp. 132-141.

25. Yuge, T., J. Heat Transfer, 81, 8, 214-220 (1960).

APPENDICES

APPENDIX A

APPENDIX A

NOTATION

B = transfer number, $c_p(T_\infty - T_s)/\lambda_A$.

Bi = Biot number, hr_o/k_a.

$\overline{C}$ = gas phase total molar concentration.

C_b = coefficient of combustion.

c_p = heat capacity of gas.

c_{pA} = heat capacity of liquid.

ΔD = distance between droplets.

D_{AB} = binary diffusion coefficient of the vapor relative to the gaseous medium.

d, d_o = droplet diameter, initial droplet diameter.

Gr = Grashof number, $g\overline{\beta}^2(T_\infty - T_s)d_o^3/\mu^2$.

g = acceleration due to gravity.

h = convective heat transfer coefficient.

k_a = thermal conductivity of air.

k_g = mass transfer coefficient.

k_m = thermal conductivity of vapor-gas mixture.

Le' = modified Lewis number, $\overline{k}_m/(\overline{D}_{AB}\overline{c}_{pA}\overline{C}\,M_m)$.

M_m = molecular weight of vapor-gas mixture.

$\dot{m}$ = mass rate of vaporization.

$\dot{m}_o$ = mass rate of vaporization in stagnant medium.

Nu = Nusselt number for heat transfer, hd/k_m.

Nu' = Nusselt number for mass transfer, $k_g M_m d(p_t - p_A)/D_{AB}\rho$.

p_A = droplet vapor pressure.

p_a = droplet vapor pressure when $T_s = T_b$.

p_t = total system pressure.

q_r = radiant heat transfer from thermocouple bead.

q_s = convective heat transfer at the surface of a thermocouple bead.

q_s^r = radiant heat flux absorbed by the droplet.

R = gas constant.

r, r_o = droplet radius, initial droplet radius.

Re = Reynolds number, $v_\infty d_o \mu/\rho$.

Sc = Schmidt number, $\mu/\rho D_{AB}$.

T_b = droplet boiling temperature.

T_c = thermocouple temperature.

T_o = initial droplet temperature.

T_s = temperature of the droplet surface.

T_w = temperature of the wall of a combustion chamber.

T_∞ = gas temperature far from the droplet.

t = time.

v_a = velocity of air stream.

v_d = velocity of droplets.

v_∞ = resultant velocity.

We = Weber number, $r_o v_\infty^2 \rho/\sigma_d$.

x_{As} = vapor mole fraction at droplet surface.

$x_{A\infty}$ = vapor mole fraction far from droplet.

$\bar{(\ )}$ = mean value of property.

α = nondimensional parameter, $\bar{c}_{pA} T_b/\lambda_A$.

β = nondimensional parameter, $\lambda_A/(RT_b)$.

$\bar{\beta}$ = coefficient of thermal expansion.

γ = droplet interaction parameter.

δ = angle of resultant velocity from horizontal.

ε = absorption coefficient for radiation.

θ_s = normalized gas phase temperature evaluated at droplet surface, T_s/T_b.

θ_∞ = normalized temperature far from the droplet, T_∞/T_b.

λ_A = latent heat of vaporization of the liquid.

μ = gas phase viscosity.

ρ = gas phase density.

ρ_ℓ = liquid phase density.

σ = Stefan-Boltzmann constant.

σ_d = surface tension of liquid.

APPENDIX B

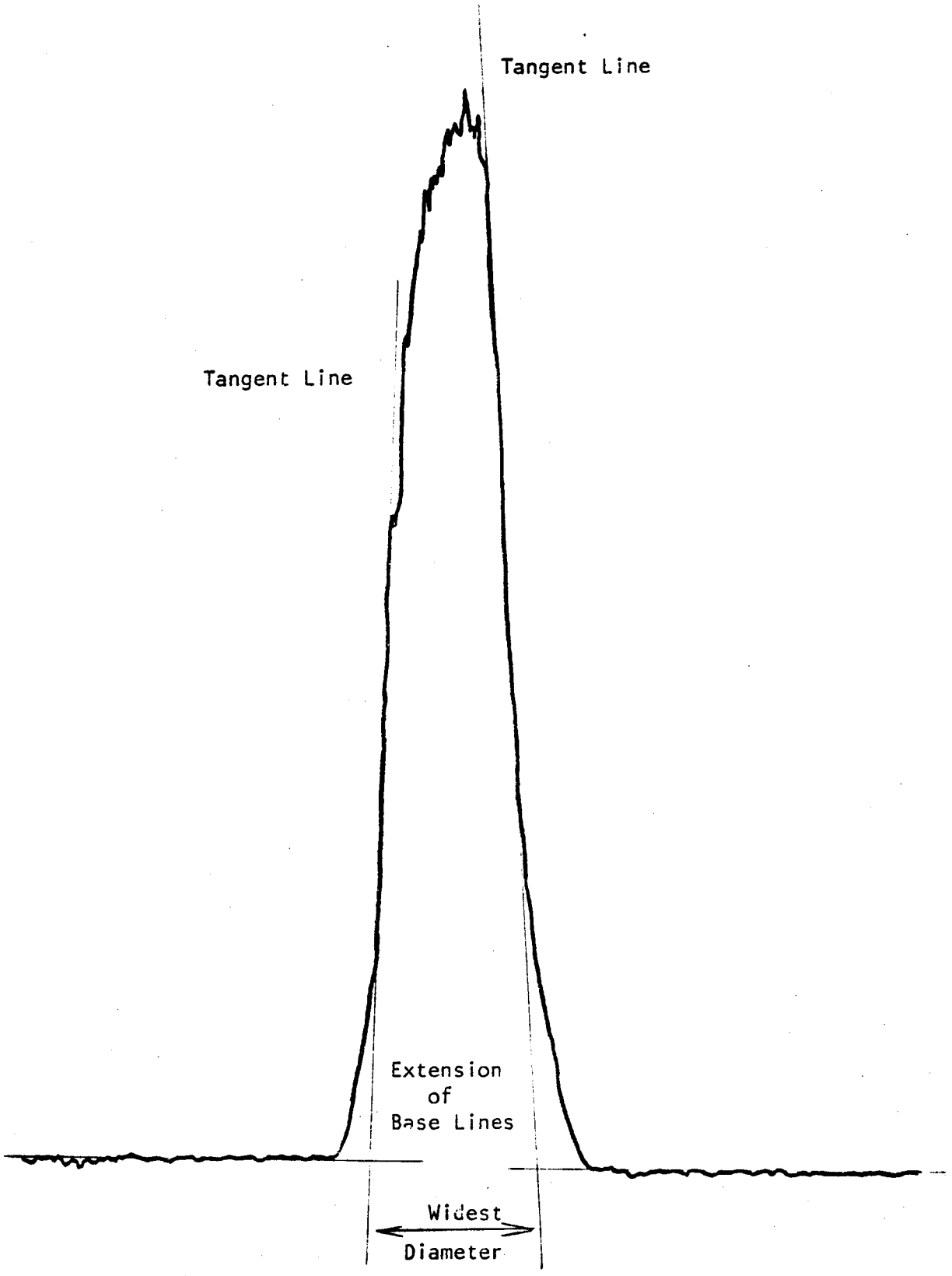

Figure 10. Microdensitometer Trace of the Wire Image

APPENDIX C

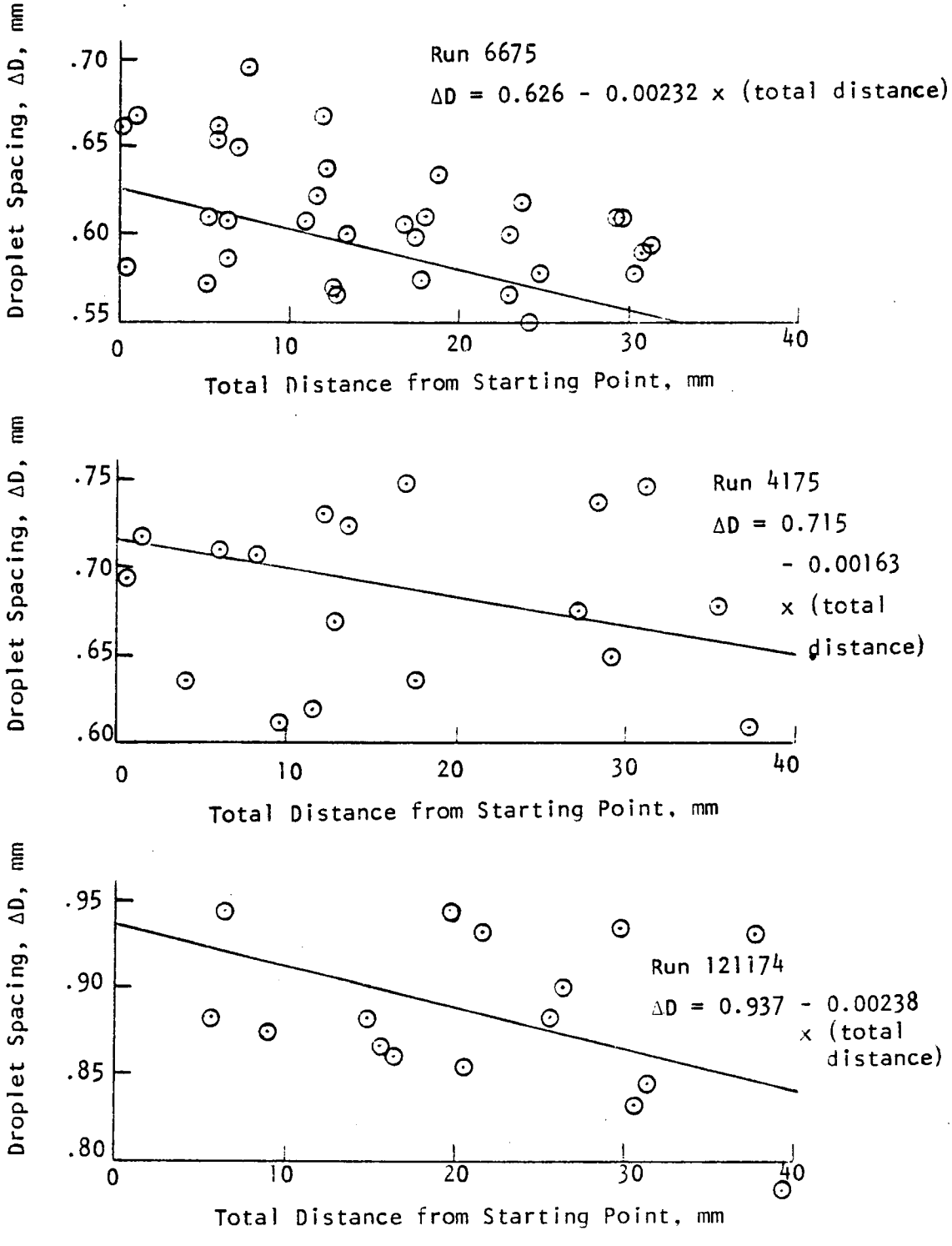

Figure 11. Droplet Spacing Correlations

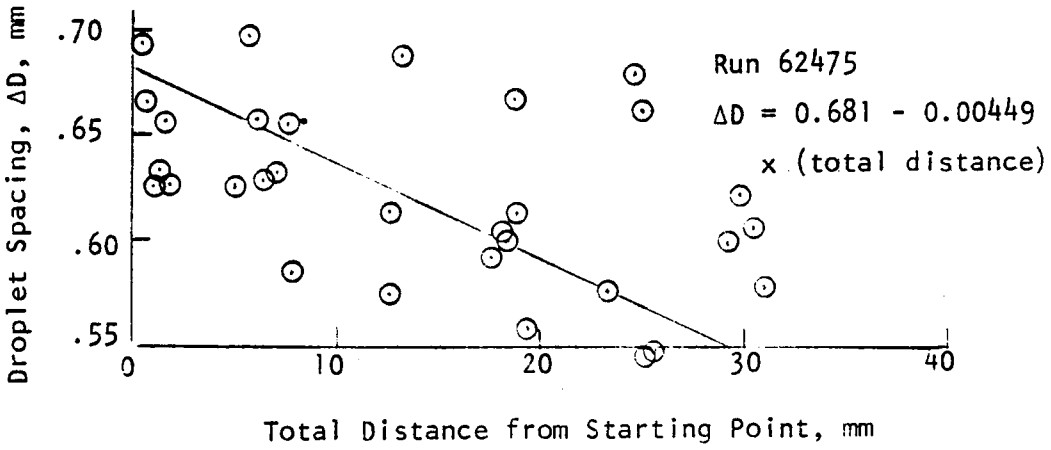

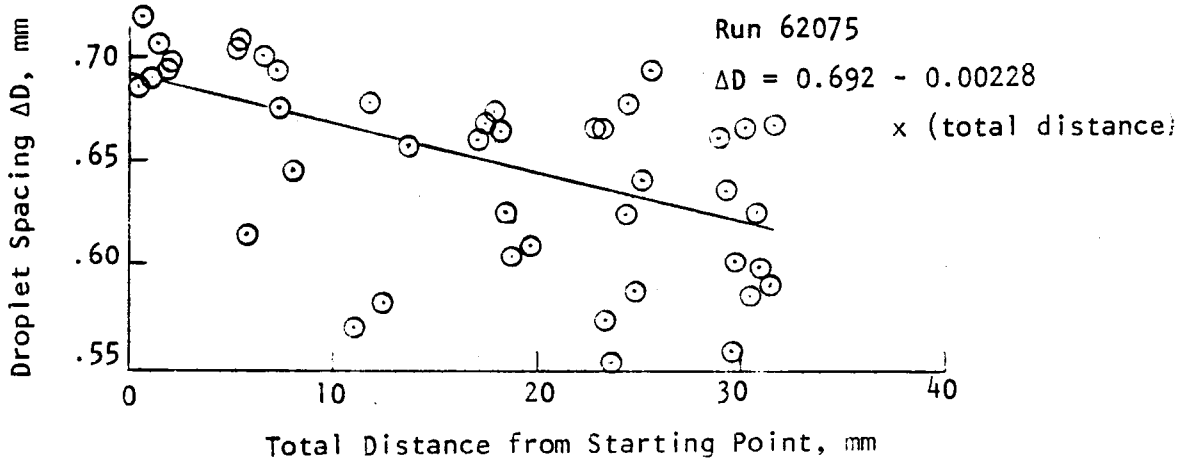

Figure 11. (continued)

APPENDIX D

TABLE 4

ADDITIONAL EXPERIMENTAL DATA

Run	Average Droplet Frequency, Drops/Min	Air Flow, l/min	Tank Pressure In Hg	Sonic Driver Frequency, Hz
121176	156316	152	9.74	2750
4175	143376	68	12.89	2570
6675	198450	102	14.31	3300
62075	202867	116	12.48	3400
62175	198545	116	15.37	3400
62475	198946	115	16.67	3300

APPENDIX E

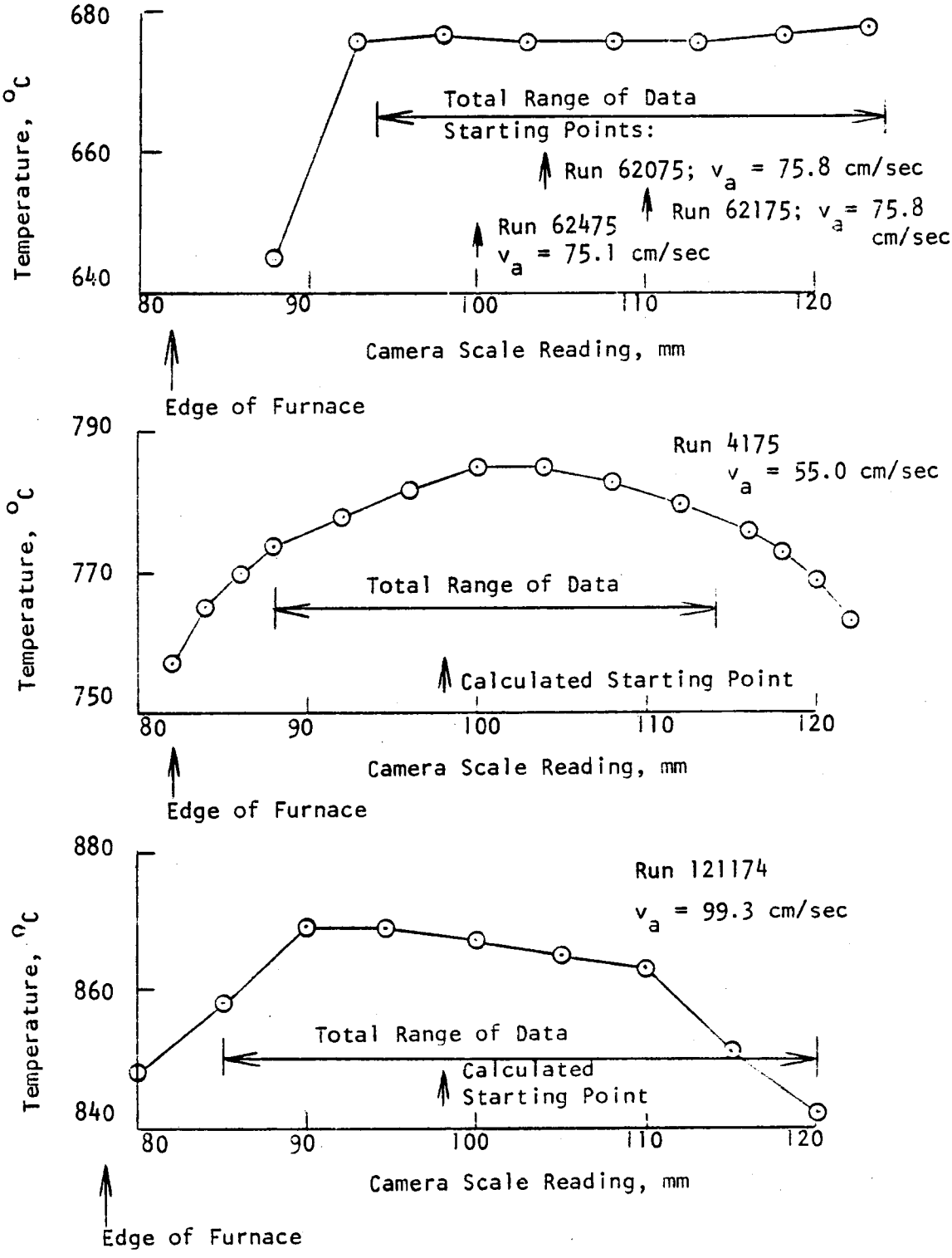

Figure 12. Temperature Profiles

VITA

Carol Lynn Mason was born in Chicago, Illinois on March 26, 1947. She moved to Indianapolis, Indiana with her family in 1950 and completed her elementary and high school education in that city, graduating from North Central High School in 1965. She attended the University of Cincinnati for two and one half years before transferring to the University of Tennessee where she graduated in March, 1970, with a Bachelor of Science degree in Chemical Engineering. Throughout her college years she was employed as a co-op student at the Oak Ridge Gaseous Diffusion Plant, Oak Ridge, Tennessee as a laboratory technician.

In March, 1970, she was employed by the Oak Ridge Gaseous Diffusion Plant as an Associate Development Engineer in the Gaseous Diffusion Development Division. Her job responsibilities included program analysis and experimental design and evaluation. After pursuing part-time graduate studies for several years, she resigned her position and returned to full-time graduate studies in January, 1975. She received a Master of Science degree in Chemical Engineering from the University of Tennessee in December, 1975. She is an associate member of the American Institute of Chemical Engineers.